Supporting Information

Content

Characterization of $[(F_5C_6)_3CO]SiCl_3$ (1a).

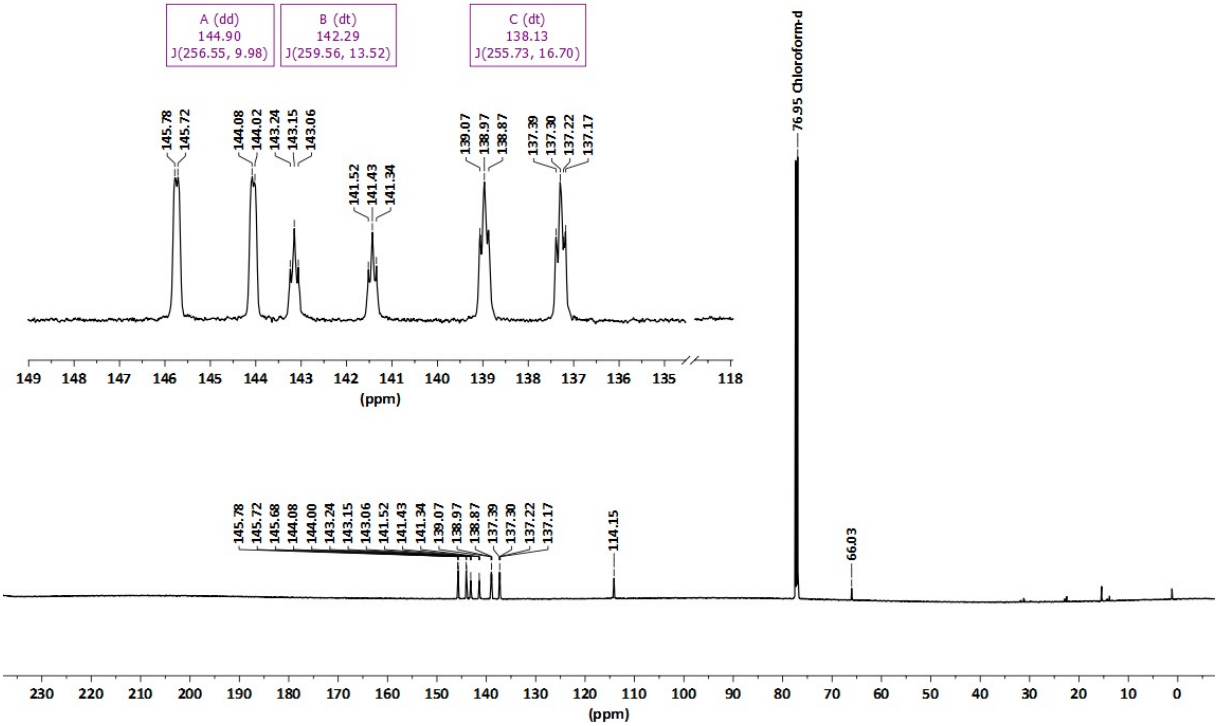

Figure S1. ^{13}C–NMR spectrum (151.0 MHz, $CDCl_3$) of $[(F_5C_6)_3CO]SiCl_3$ (**1a**).

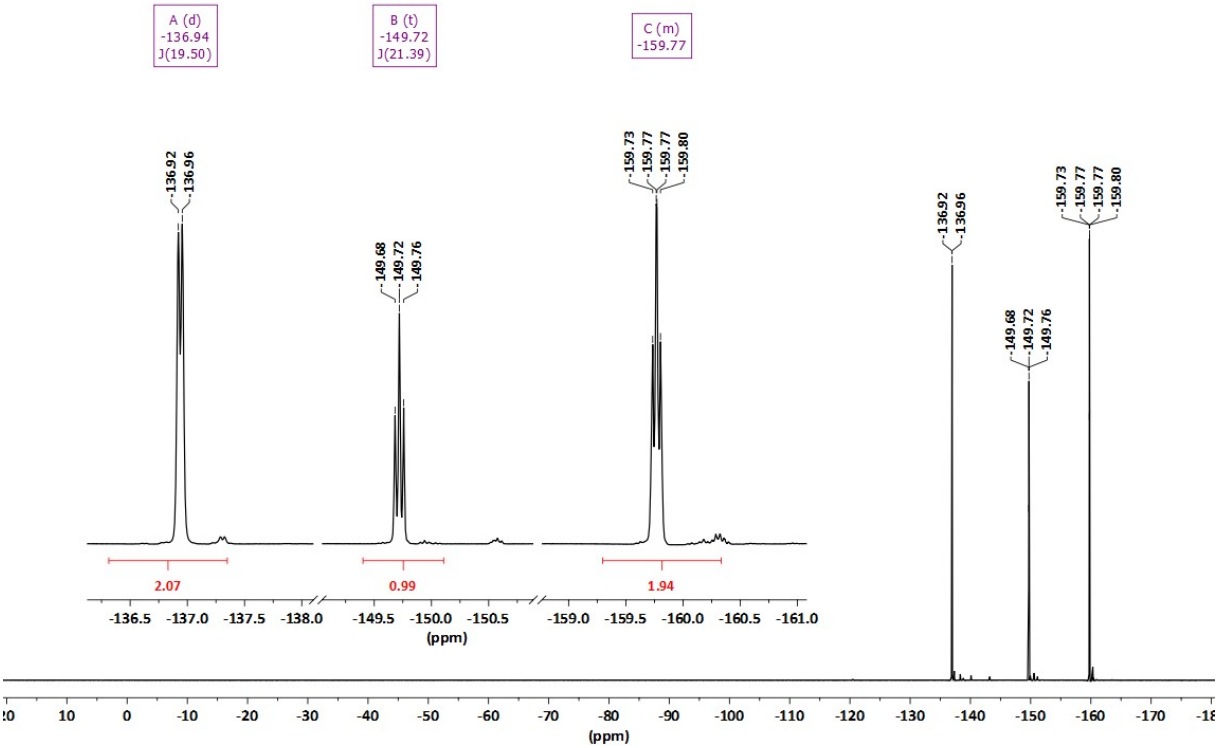

Figure S2. ^{19}F–NMR spectrum (564.7 MHz, $CDCl_3$) of $[(F_5C_6)_3CO]SiCl_3$ (**1a**).

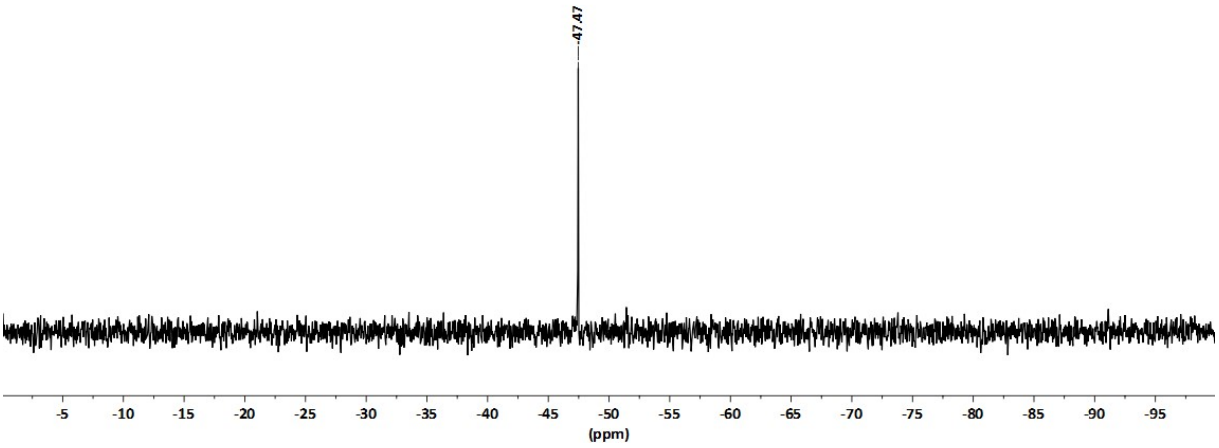

Figure S3. $^{29}Si–\{^{1}H\}–NMR$ spectrum (119.3 MHz, $CDCl_3$) of $[(F_5C_6)_3CO]SiCl_3$ (**1a**).

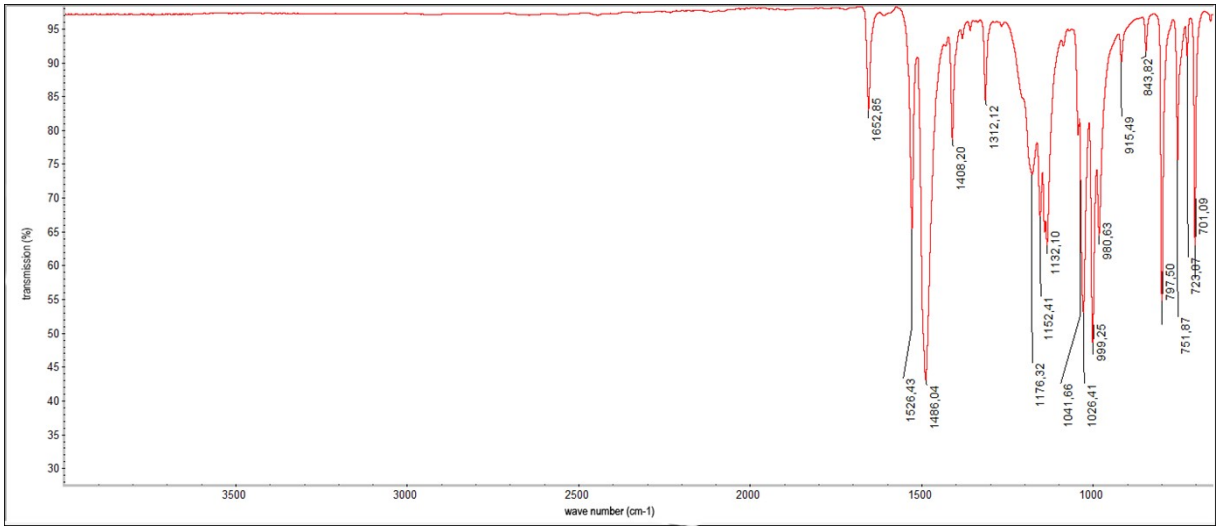

Figure S4. IR spectrum (neat) of $[(F_5C_6)_3CO]SiCl_3$ (**1a**).

Characterization of {[3,5-$(CF_3)_2C_6H_3$]$_3$CO}$SiCl_3$ (1b).

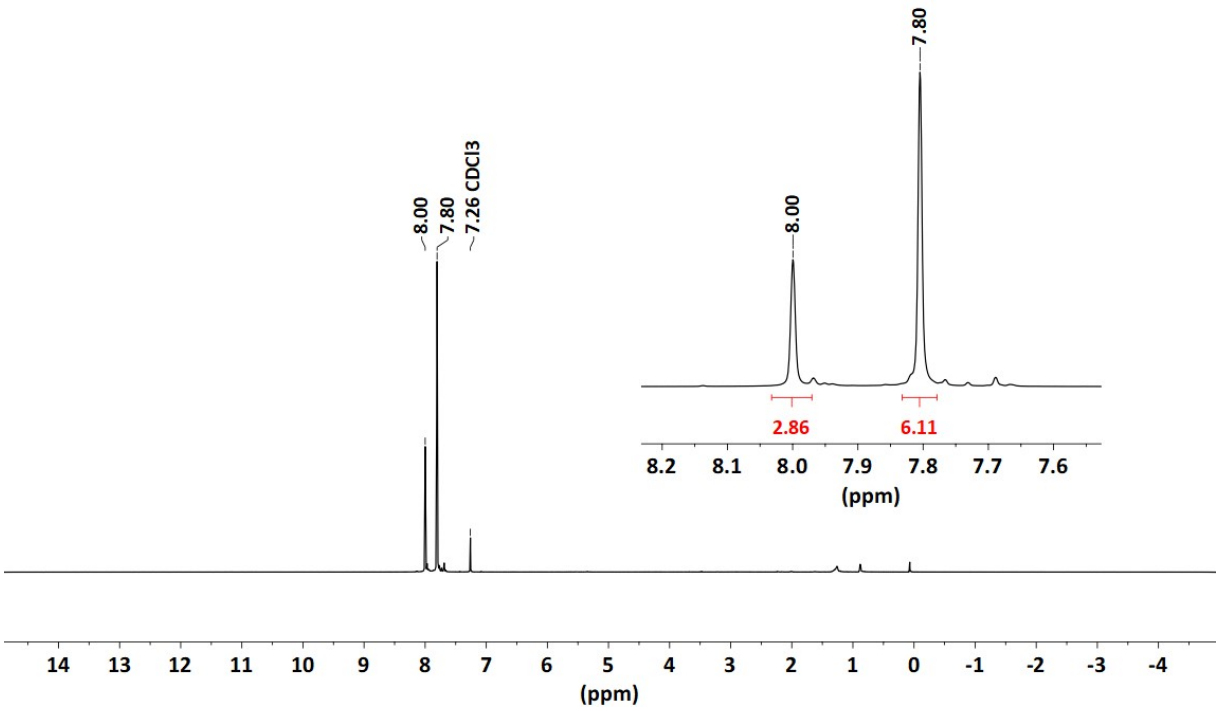

Figure S5. ^{1}H–NMR spectrum (600.2 MHz, $CDCl_3$) of {[3,5-$(CF_3)_2C_6H_3$]$_3$CO}$SiCl_3$ (**1b**).

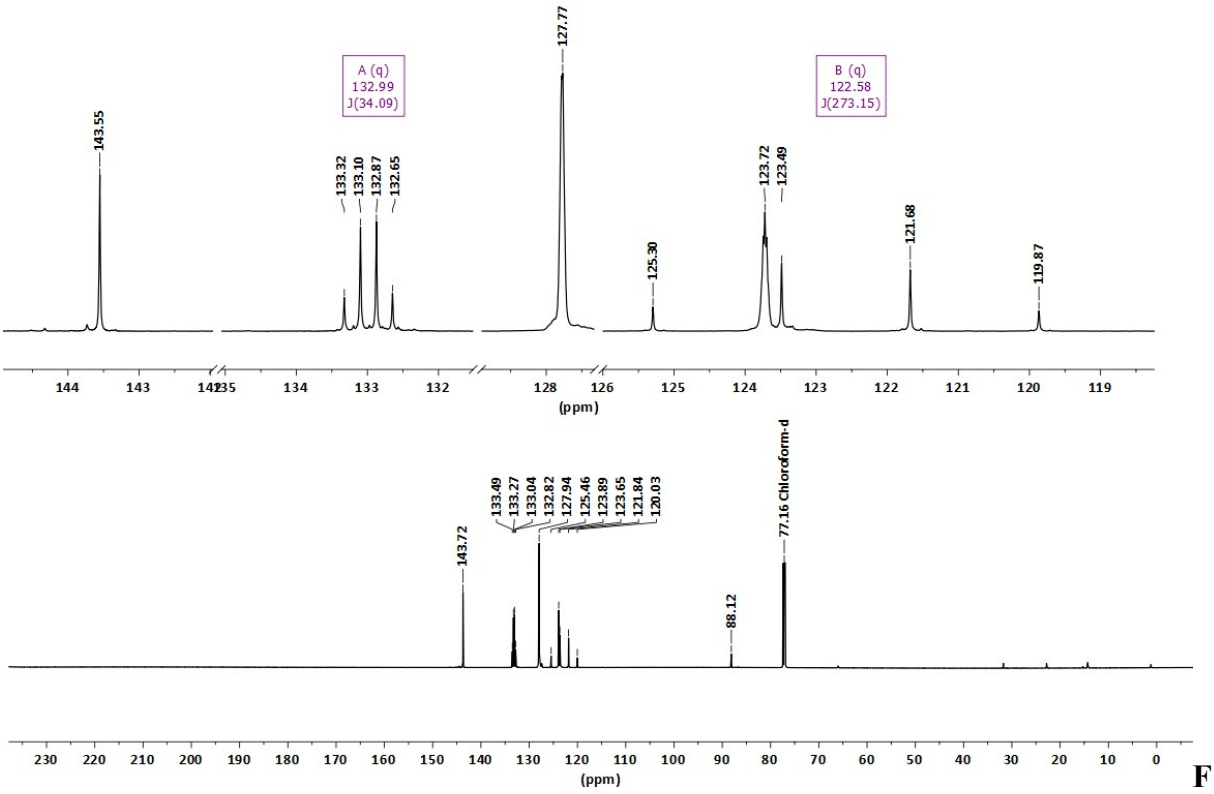

Figure S6. $^{13}C–\{^{1}H\}–NMR$ spectrum (151.0 MHz, $CDCl_3$) of $\{[3,5\text{-}(CF_3)_2C_6H_3]_3CO\}SiCl_3$ (**1b**).

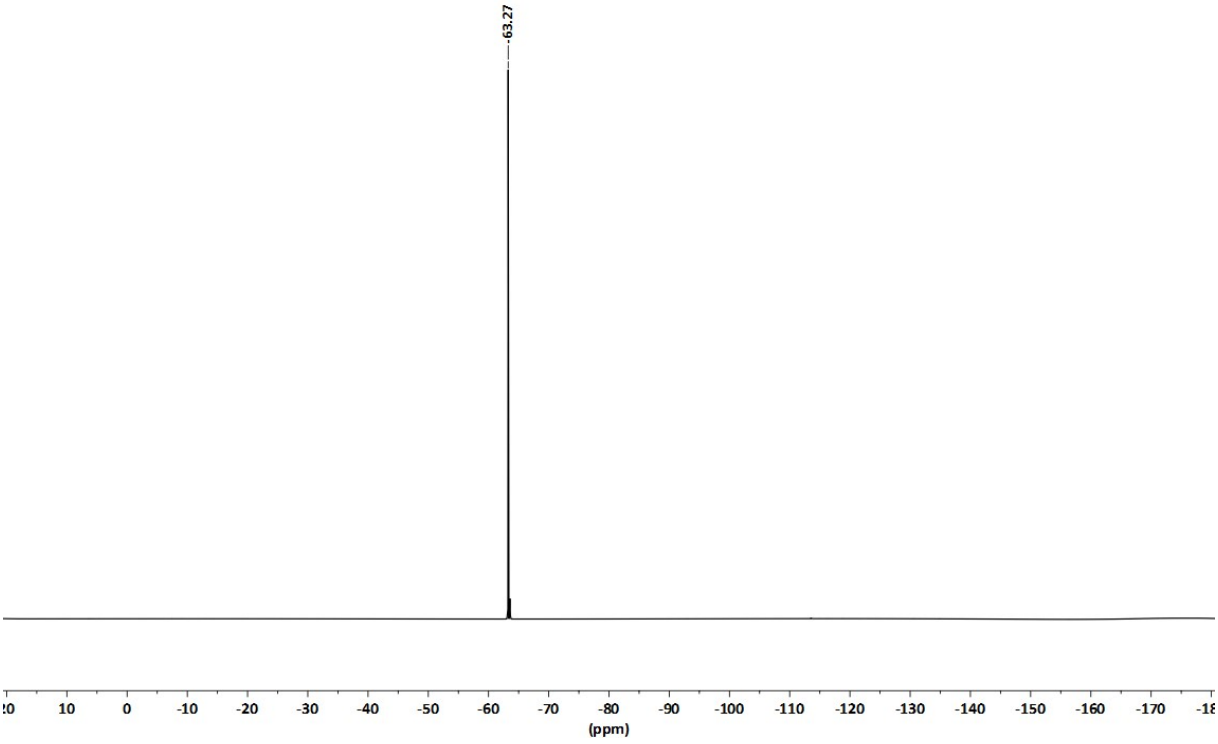

Figure S7. $^{19}F–NMR$ spectrum (564.7 MHz, $CDCl_3$) of $\{[3,5\text{-}(CF_3)_2C_6H_3]_3CO\}SiCl_3$ (**1b**).

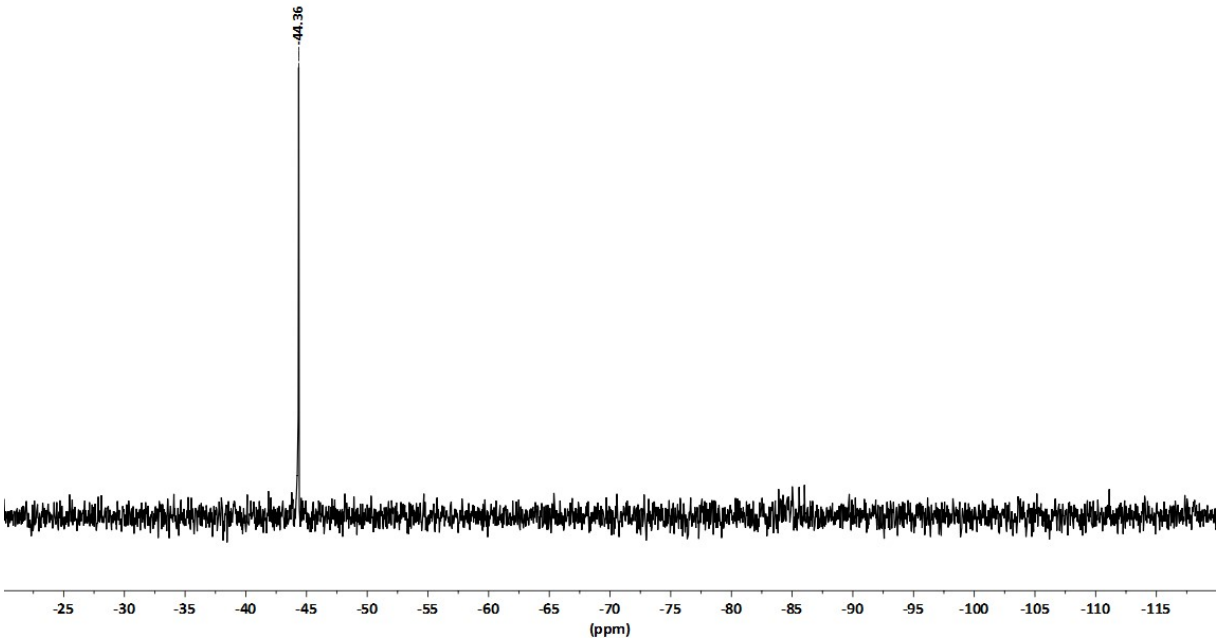

Figure S8. $^{29}Si–\{^{1}H\}–NMR$ spectrum (119.3 MHz, $CDCl_3$) of $\{[3,5\text{-}(CF_3)_2C_6H_3]_3CO\}SiCl_3$ (**1b**).

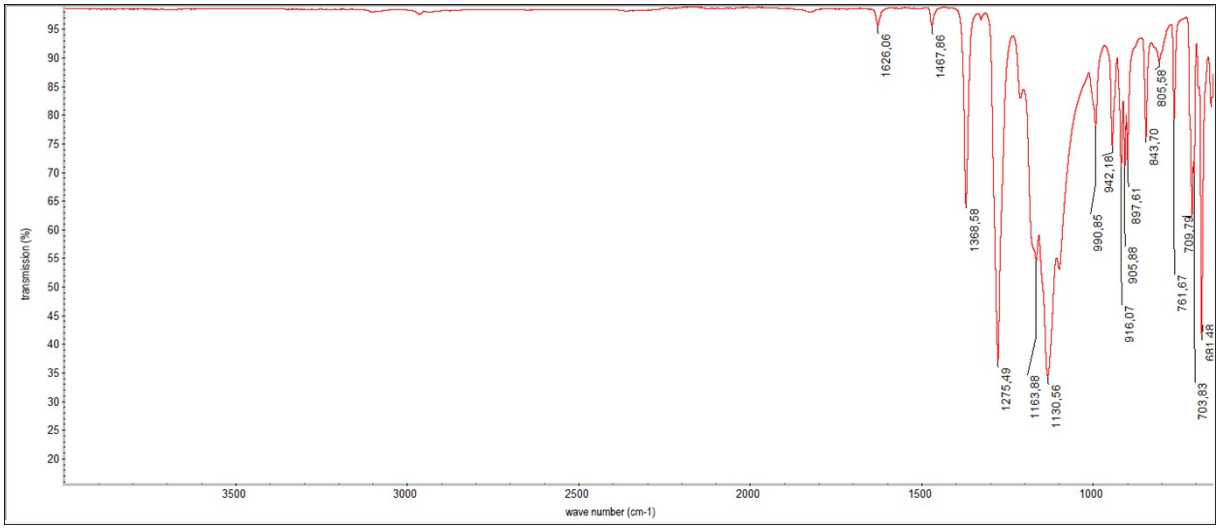

Figure S9. IR spectrum (neat) of $\{[3,5\text{-}(CF_3)_2C_6H_3]_3CO\}SiCl_3$ (**1b**).

Characterization of $[(F_5C_6)_3CO]Si(OH)_3$ (2a).

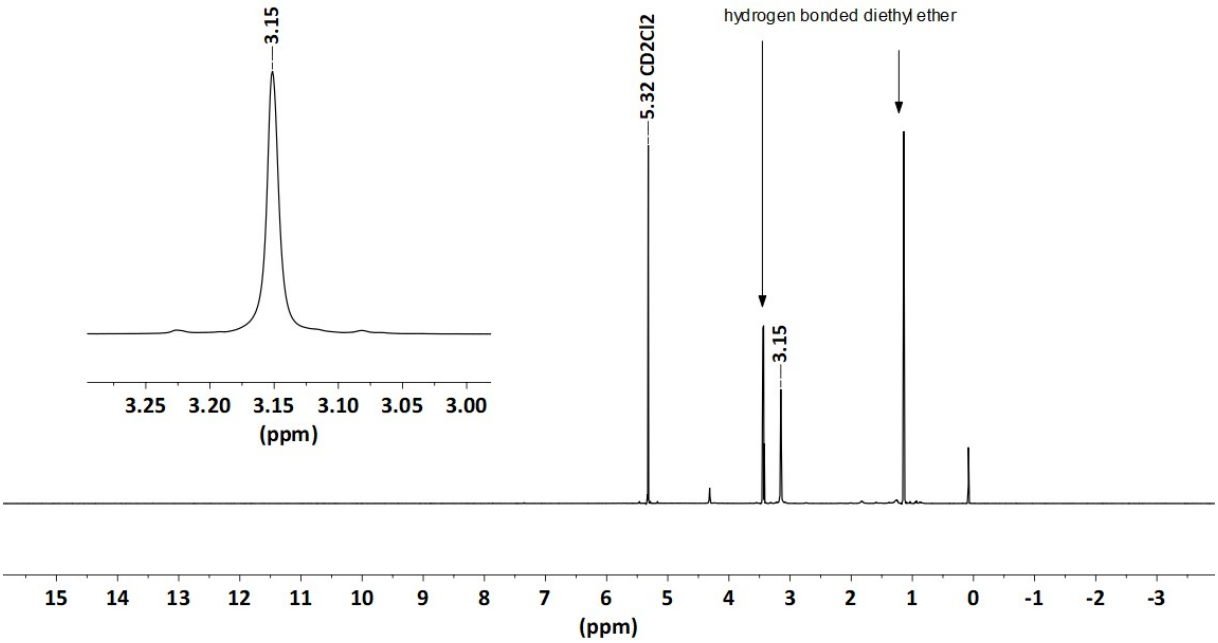

Figure S10. ^{1}H–NMR spectrum (600.2 MHz, CD_2Cl_2) of $[(F_5C_6)_3CO]Si(OH)_3$ (**2a**).

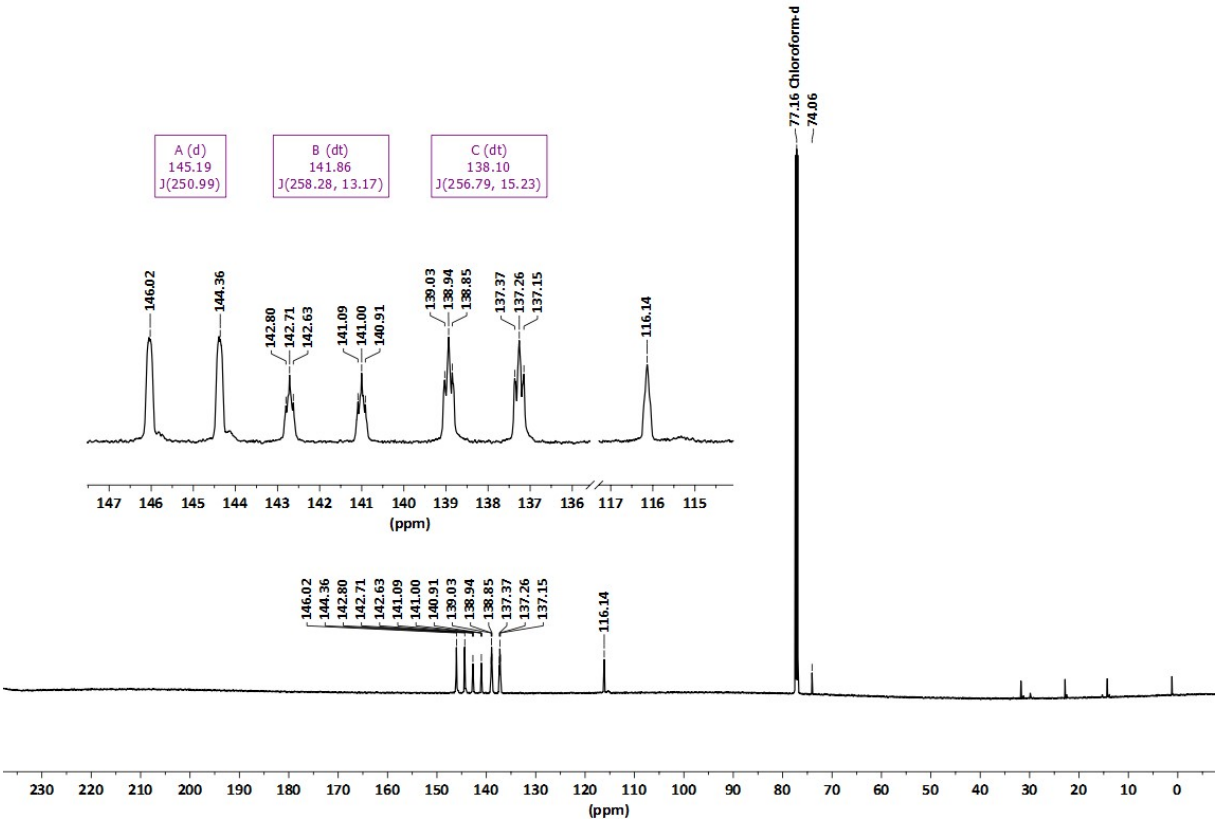

Figure S11. ^{13}C–{^{1}H}–NMR spectrum (150.9 MHz, $CDCl_3$) of $[(F_5C_6)_3CO]Si(OH)_3$ (**2a**).

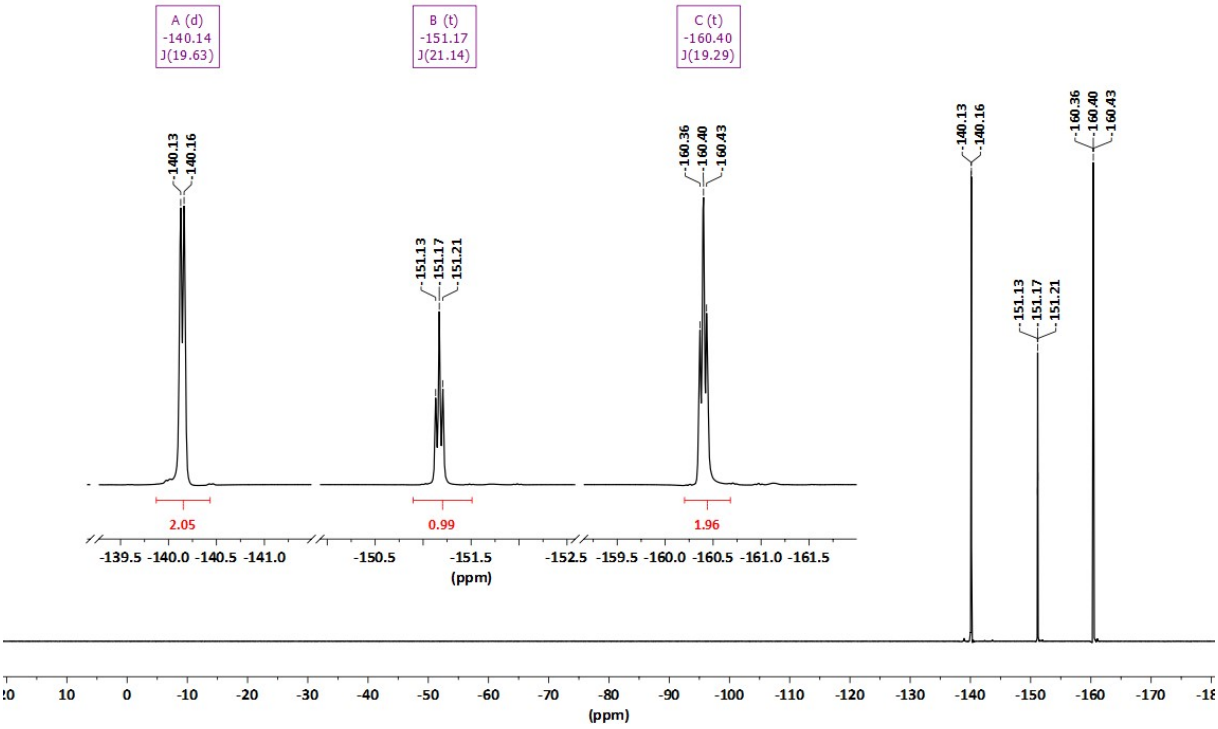

Figure S12. ^{19}F–NMR spectrum (564.7 MHz, $CDCl_3$) of $[(F_5C_6)_3CO]Si(OH)_3$ (**2a**).

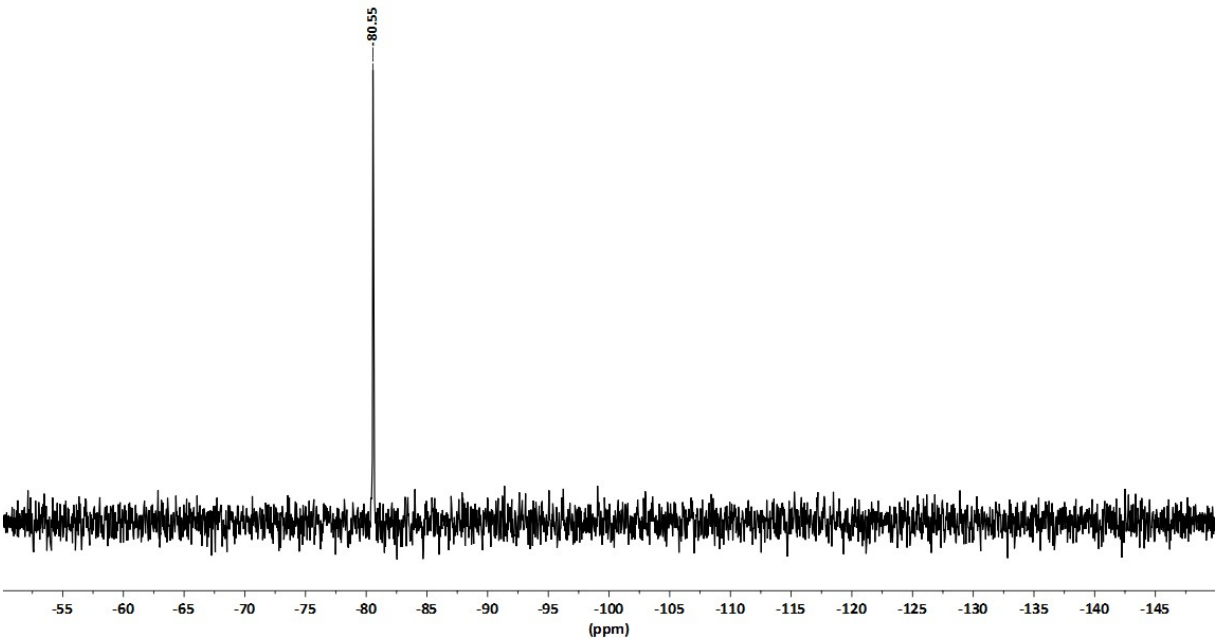

Figure S13. ^{29}Si–$\{^1H\}$–NMR spectrum (119.3 MHz, $CDCl_3$) of $[(F_5C_6)_3CO]Si(OH)_3$ (**2a**).

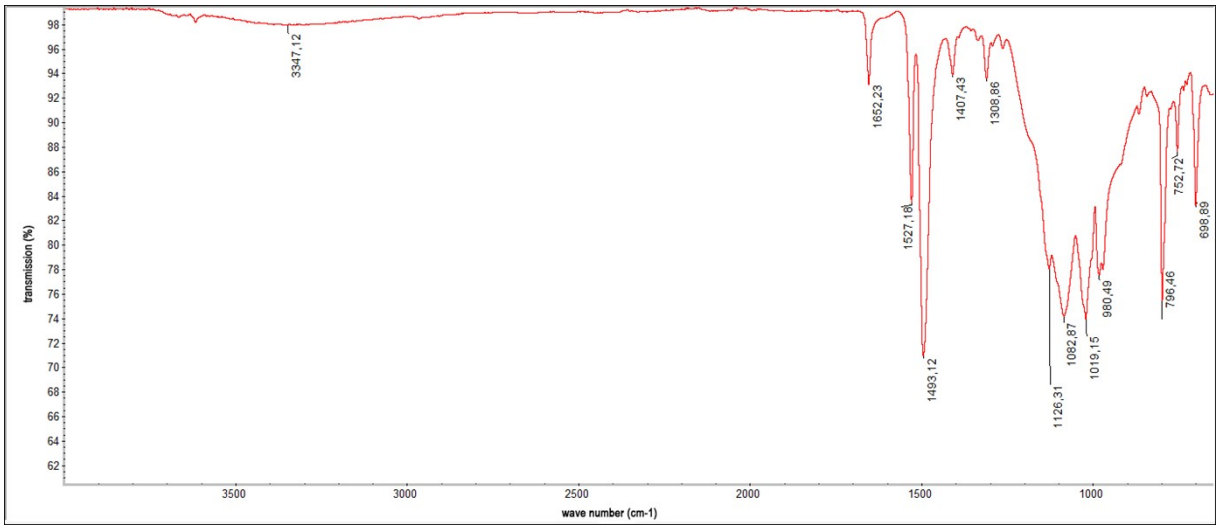

Figure S14. IR spectrum (neat) of $[(F_5C_6)_3CO]Si(OH)_3$ (**2a**).

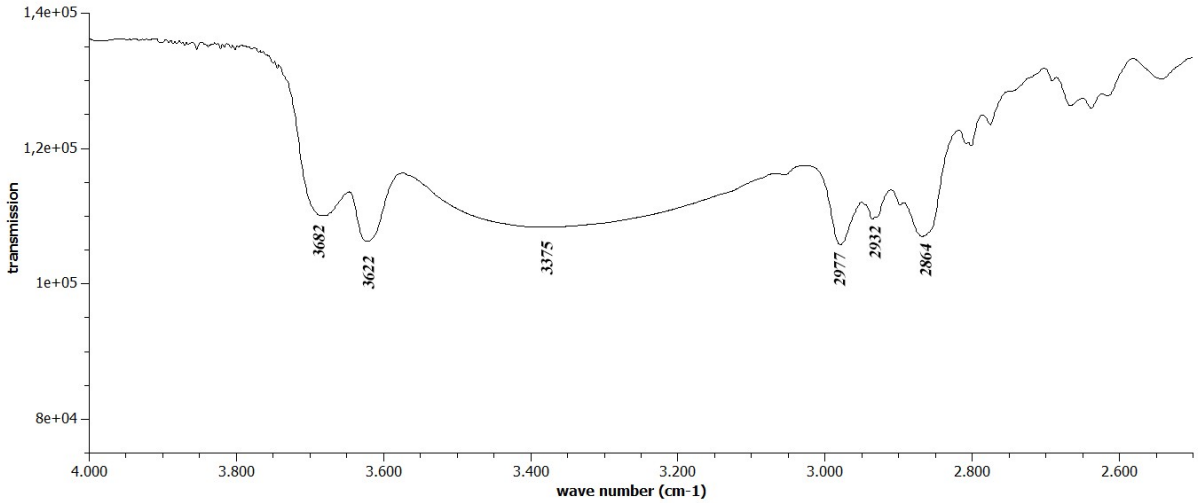

Figure S15. IR spectrum (sample dissolved in CCl_4, c = 20 mg mL^{-1}) of $[(F_5C_6)_3CO]Si(OH)_3$ (**2a**).

Characterization of $\{[3,5\text{-}(CF_3)_2C_6H_3]_3CO\}Si(OH)_3$ (2b).

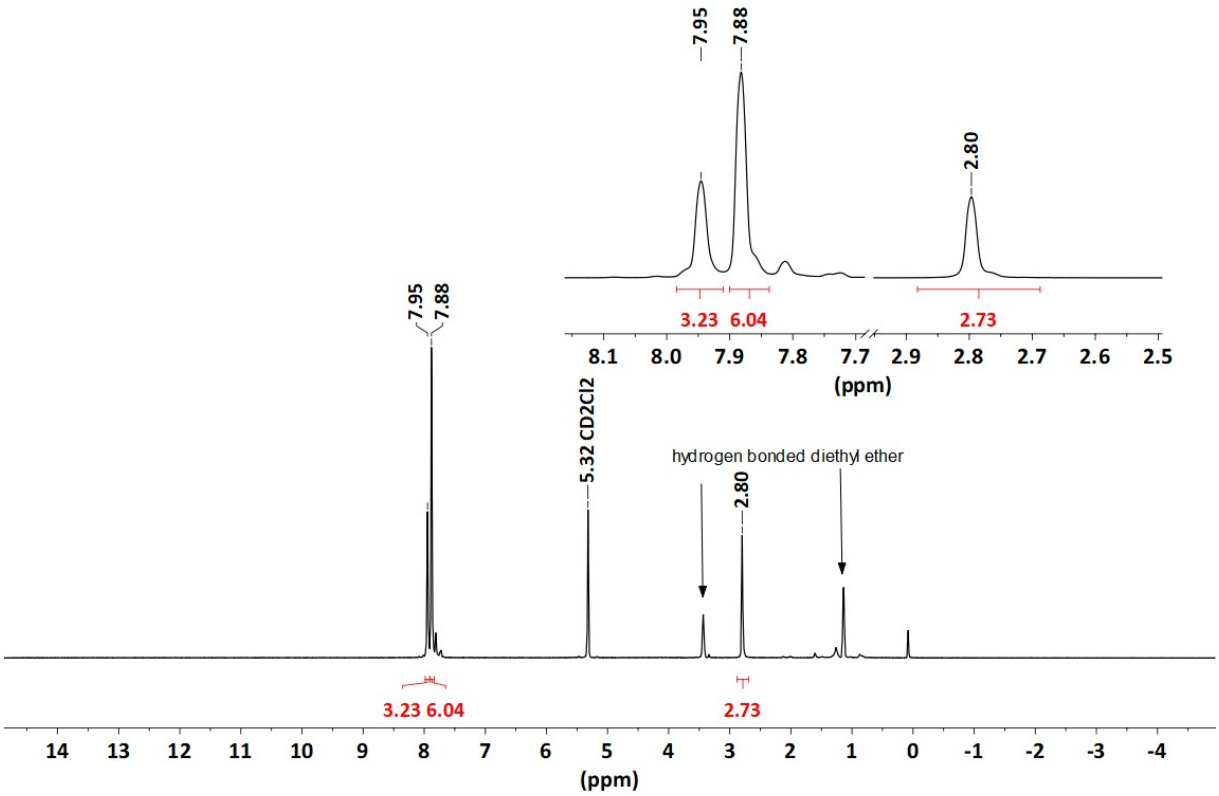

Figure S16. ^{1}H–NMR spectrum (600.2 MHz, CD_2Cl_2) of $\{[3,5\text{-}(CF_3)_2C_6H_3]_3CO\}Si(OH)_3$ (**2b**).

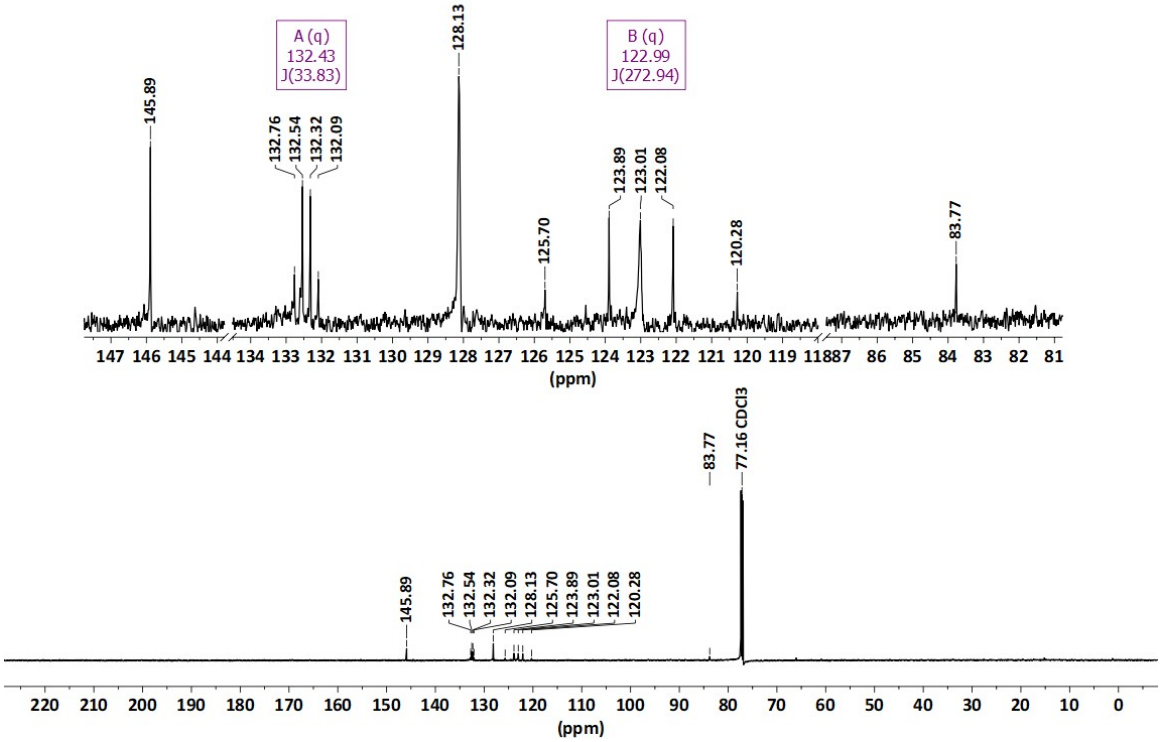

Figure S17. $^{13}C–\{^{1}H\}–NMR$ spectrum (150.9 MHz, $CDCl_3$) of $\{[3,5\text{-}(CF_3)_2C_6H_3]_3CO\}Si(OH)_3$ (**2b**).

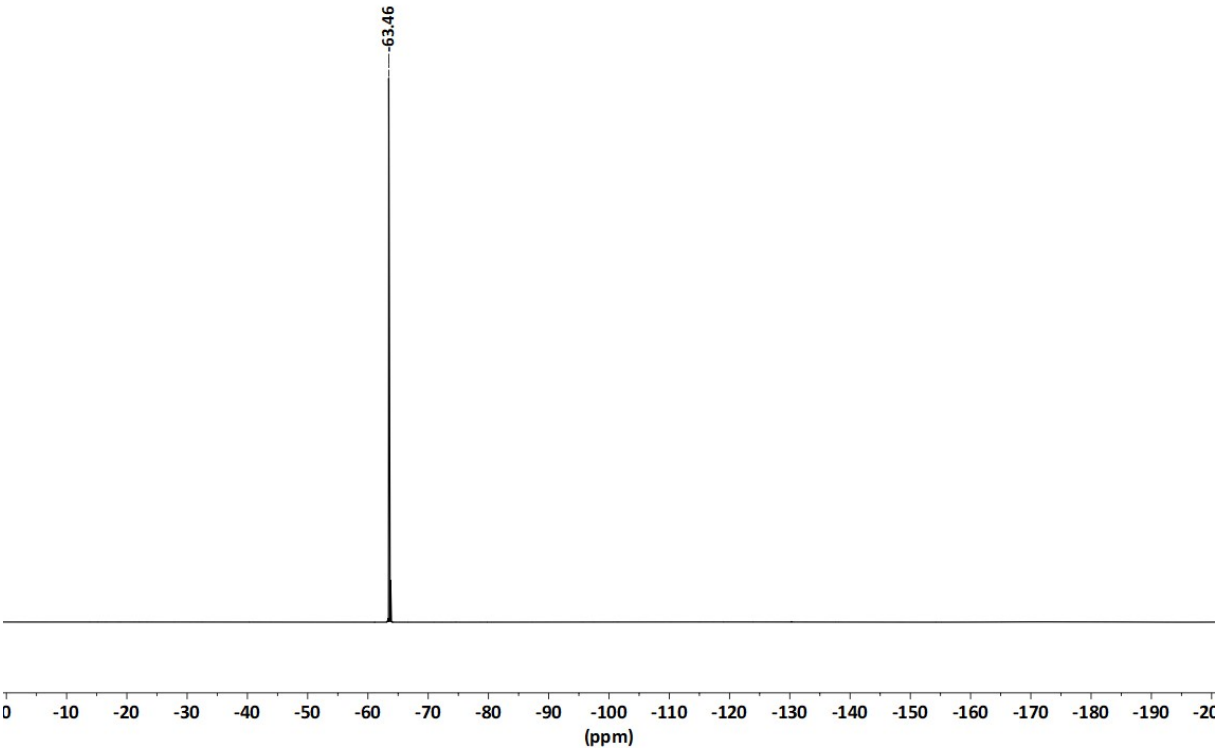

Figure S18. $^{19}F–NMR$ spectrum (564.7 MHz, $CDCl_3$) of $\{[3,5\text{-}(CF_3)_2C_6H_3]_3CO\}Si(OH)_3$ (**2b**).

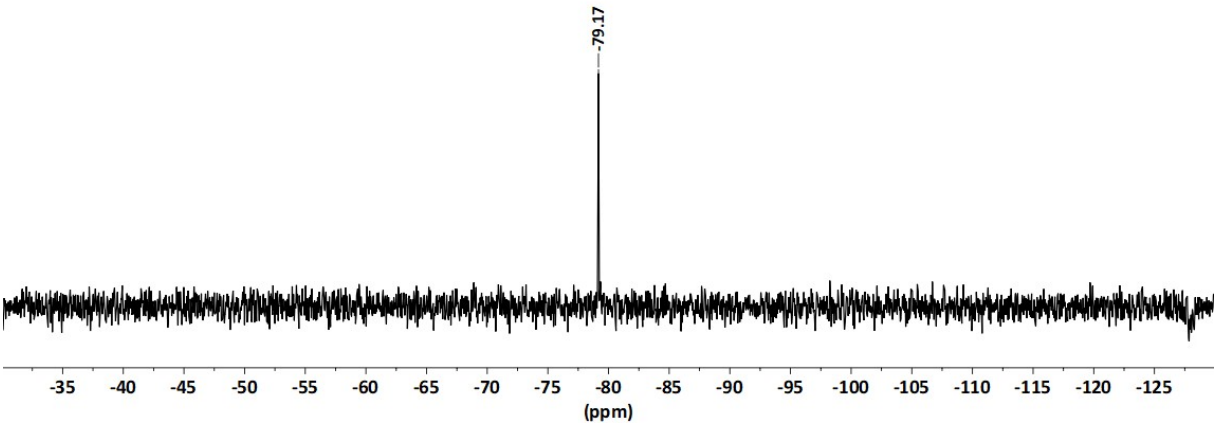

Figure S19. $^{29}Si–\{^{1}H\}–NMR$ spectrum (119.3 MHz, $CDCl_3$) of $\{[3,5\text{-}(CF_3)_2C_6H_3]_3CO\}Si(OH)_3$ (**2b**).

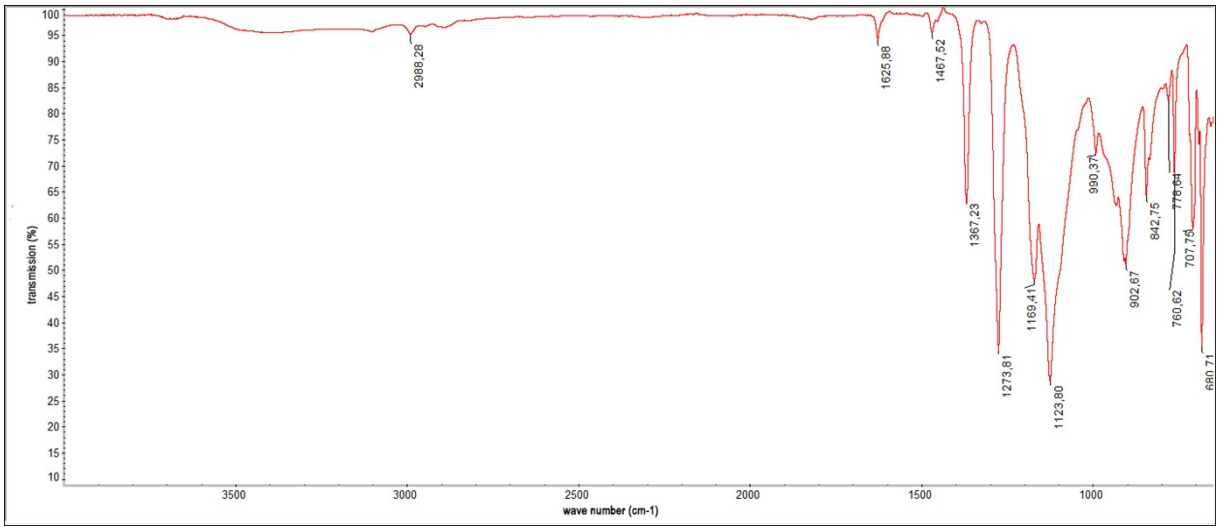

Figure S20. IR spectrum (neat) of $\{[3,5\text{-}CF_3)_2C_6H_3]_3CO\}Si(OH)_3$ (**2b**).

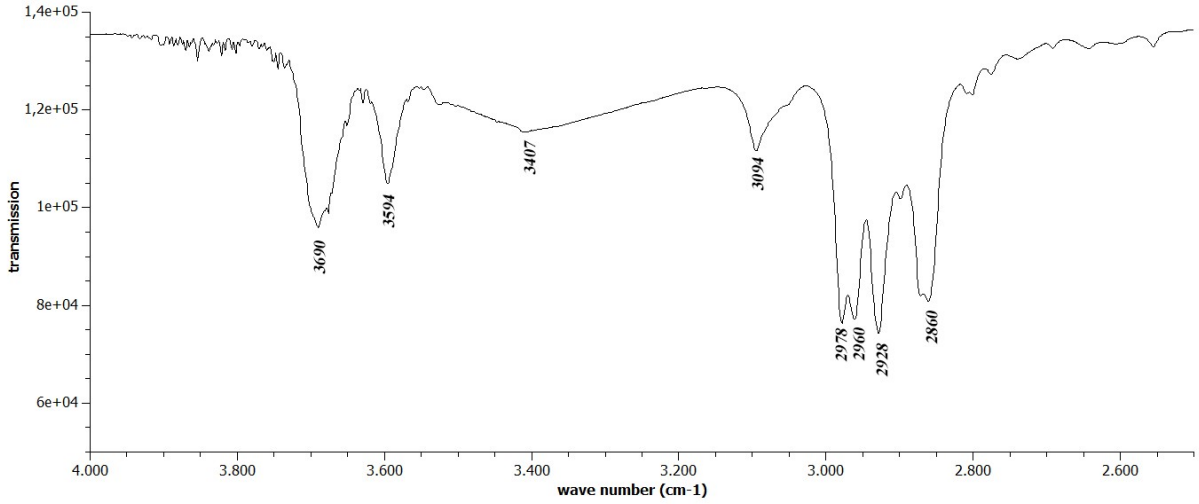

Figure S21. IR spectrum (sample dissolved in CCl_4, c = 20 mg mL^{-1}) of $\{[3,5\text{-}(CF_3)_2C_6H_3]_3CO\}Si(OH)_3$ (**2b**).

Characterization of $\{[(F_5C_6)_3CO]SiCl_2\}_2O$ (3a).

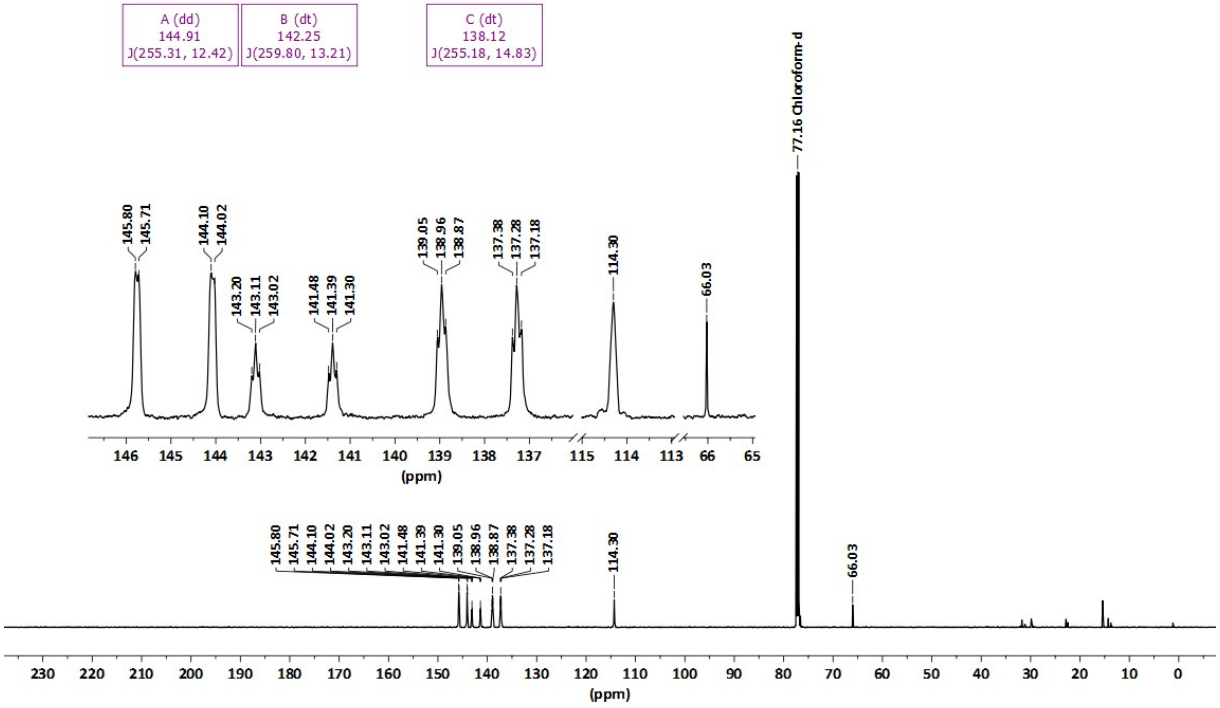

Figure S22. $^{13}C–\{^{1}H\}–NMR$ spectrum (151.0 MHz, $CDCl_3$) of $\{[(F_5C_6)_3CO]SiCl_2\}_2O$ (**3a**).

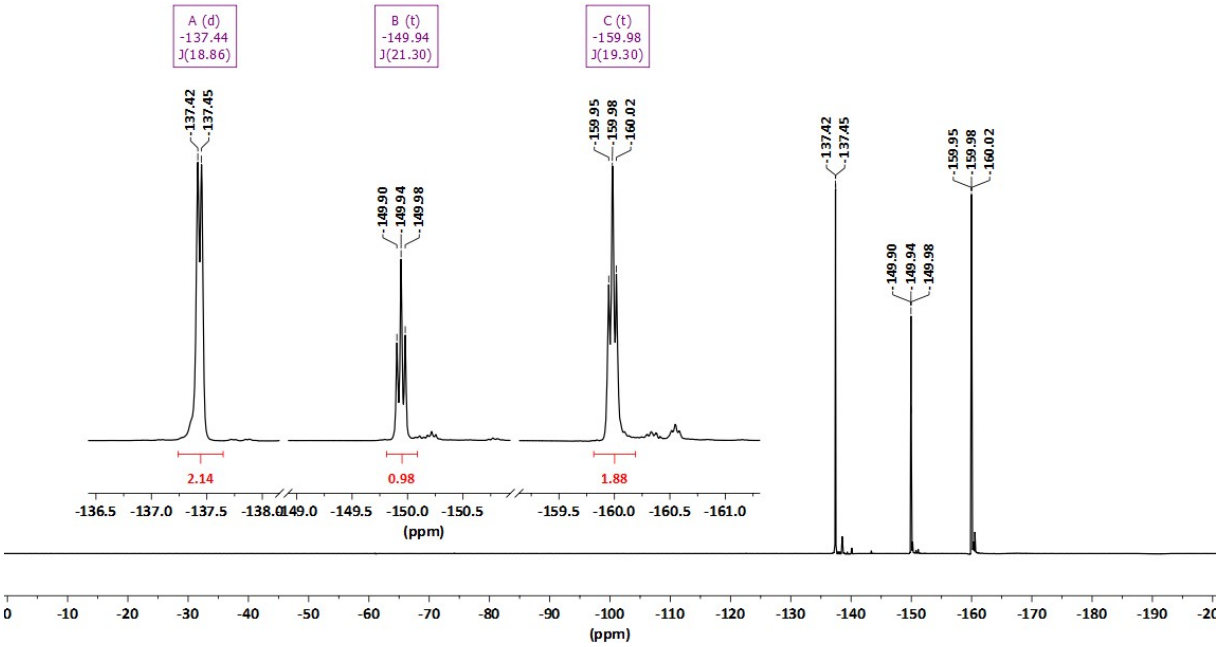

Figure S23. $^{19}F–NMR$ spectrum (564.7 MHz, $CDCl_3$) of $\{[(F_5C_6)_3CO]SiCl_2\}_2O$ (**3a**).

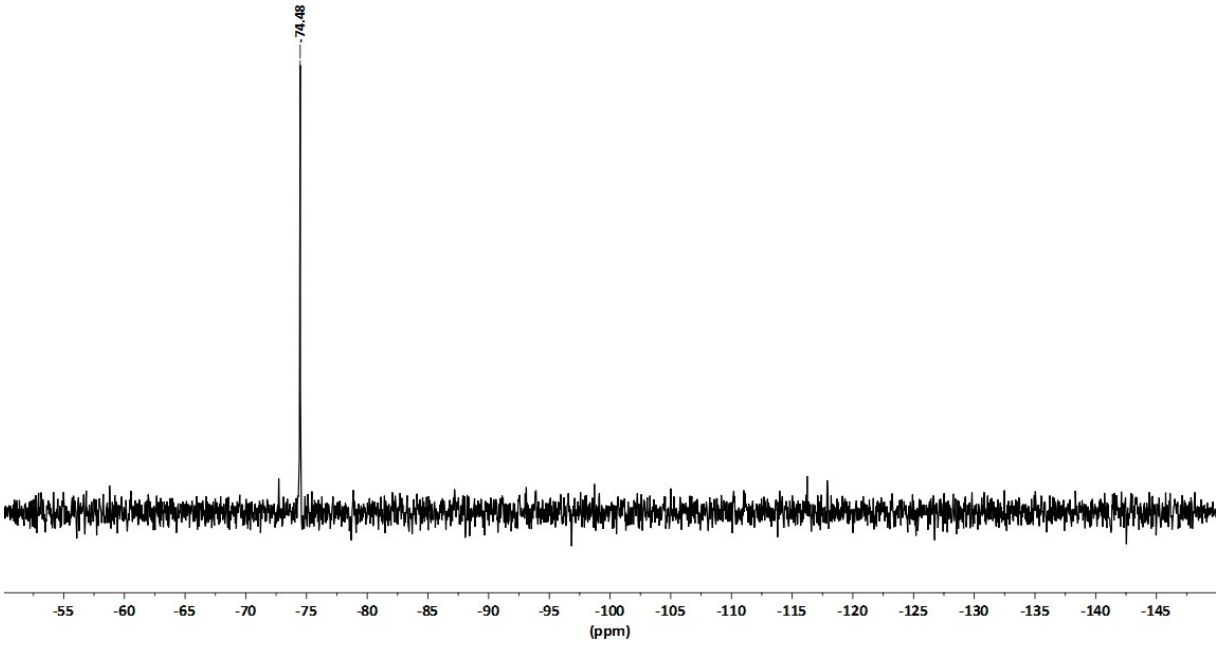

Figure S24. $^{29}Si–\{^{1}H\}–NMR$ spectrum (119.3 MHz, $CDCl_3$) of $\{[(F_5C_6)_3CO]SiCl_2\}_2O$ (**3a**).

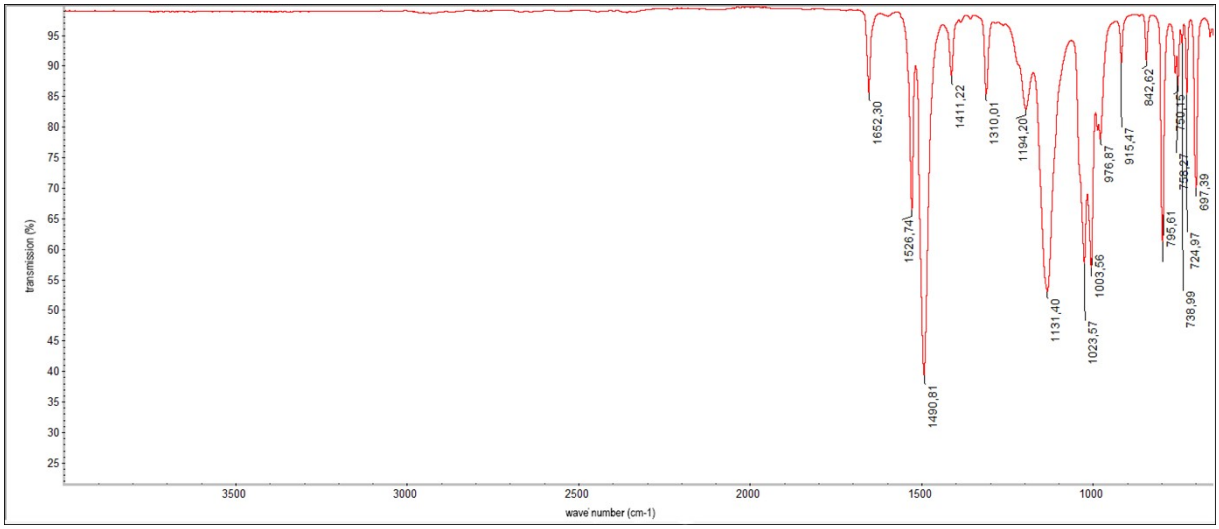

Figure S25. IR spectrum (neat) of $\{[(F_5C_6)_3CO]SiCl_2\}_2O$ (**3a**).

Characterization of {[(3,5-$(CF_3)_2C_6H_3)_3CO$]$SiCl_2$}$_2$O (3b).

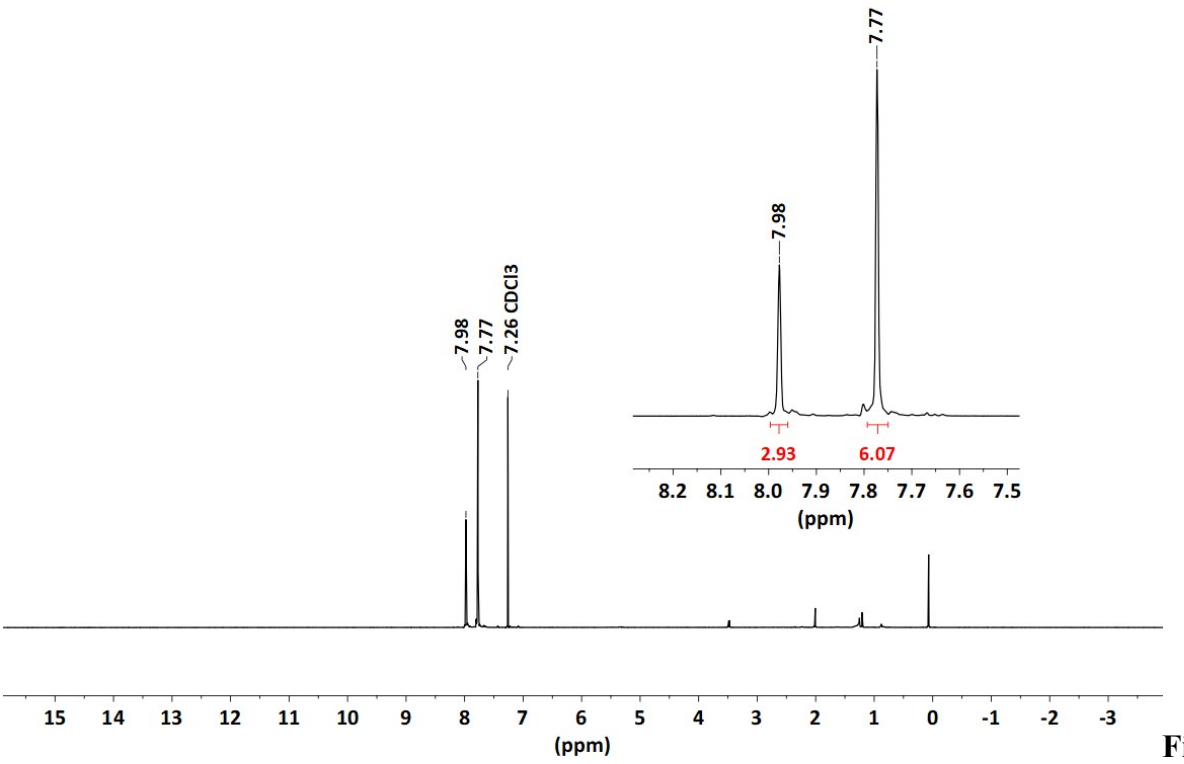

Figure S26. ^{1}H–NMR spectrum (600.2 MHz, $CDCl_3$) of {[(3,5-$(CF_3)_2C_6H_3)_3CO$]$SiCl_2$}$_2$O (**3b**).

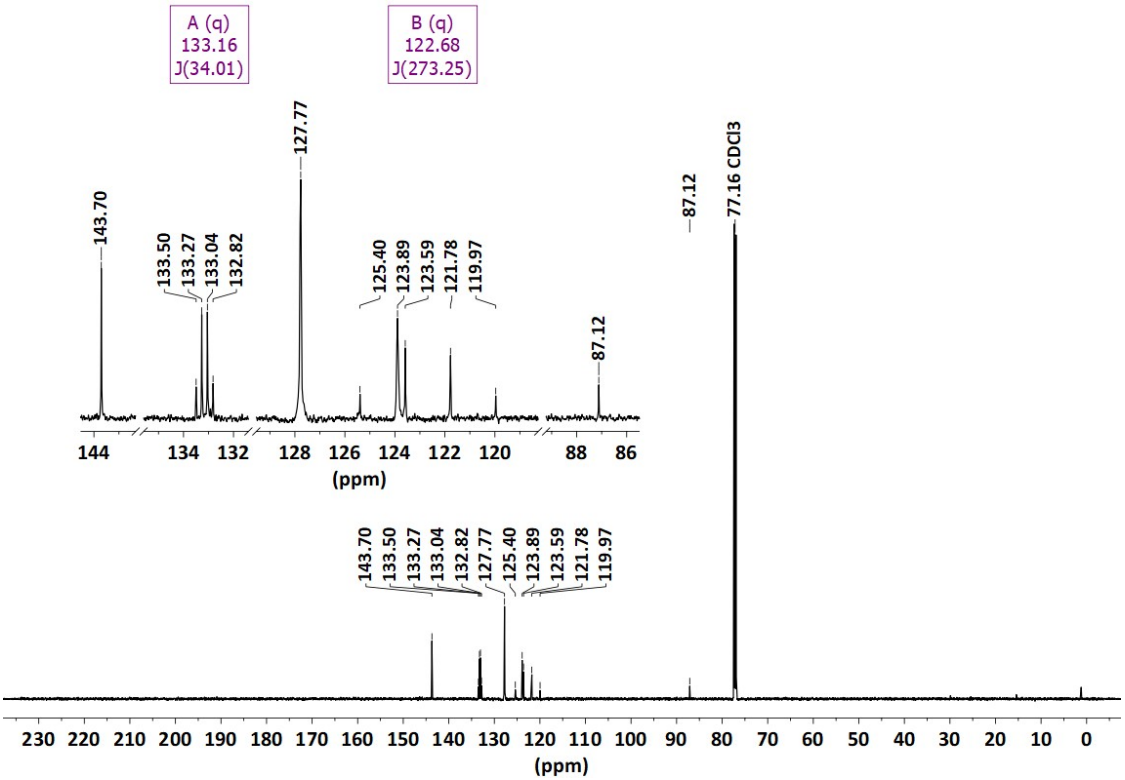

Figure S27. $^{13}C–\{^{1}H\}–NMR$ spectrum (150.9 MHz, $CDCl_3$) of $\{[(3,5\text{-}(CF_3)_2C_6H_3)_3CO]SiCl_2\}_2O$ (**3b**).

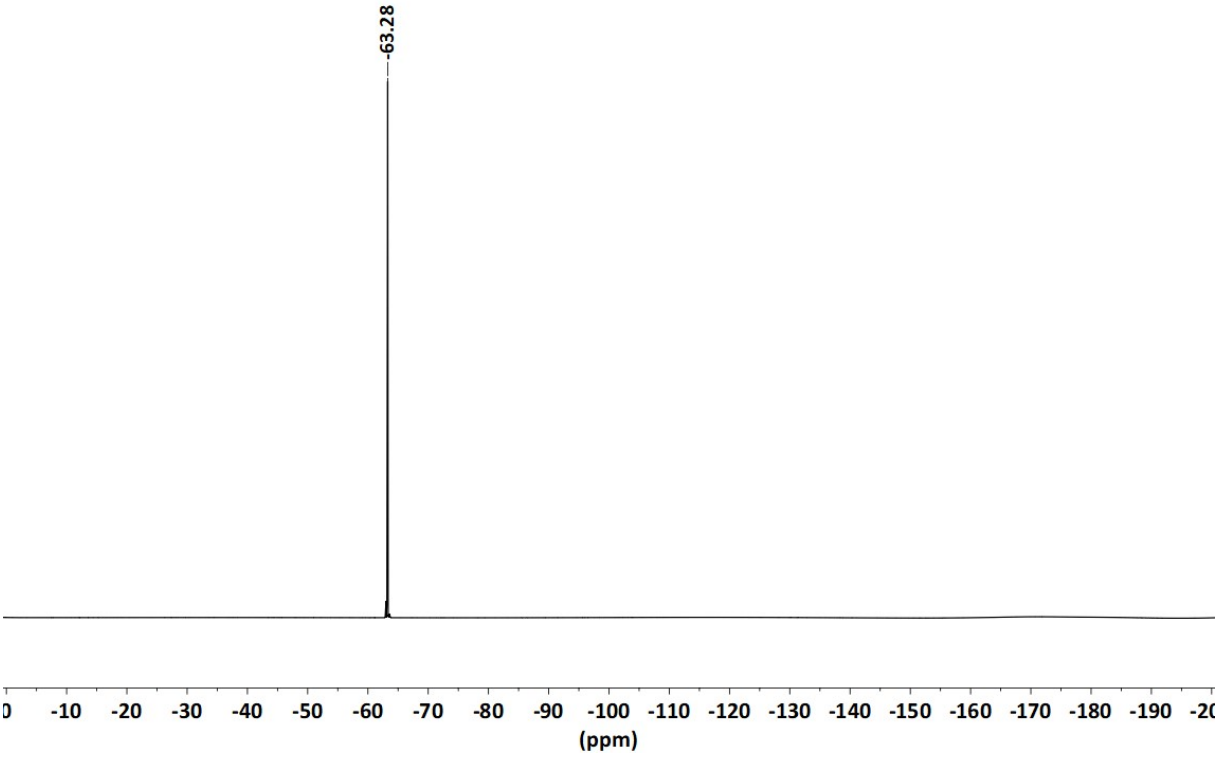

Figure S28. $^{19}F–NMR$ spectrum (564.7 MHz, $CDCl_3$) of $\{[(3,5\text{-}(CF_3)_2C_6H_3)_3CO]SiCl_2\}_2O$ (**3b**).

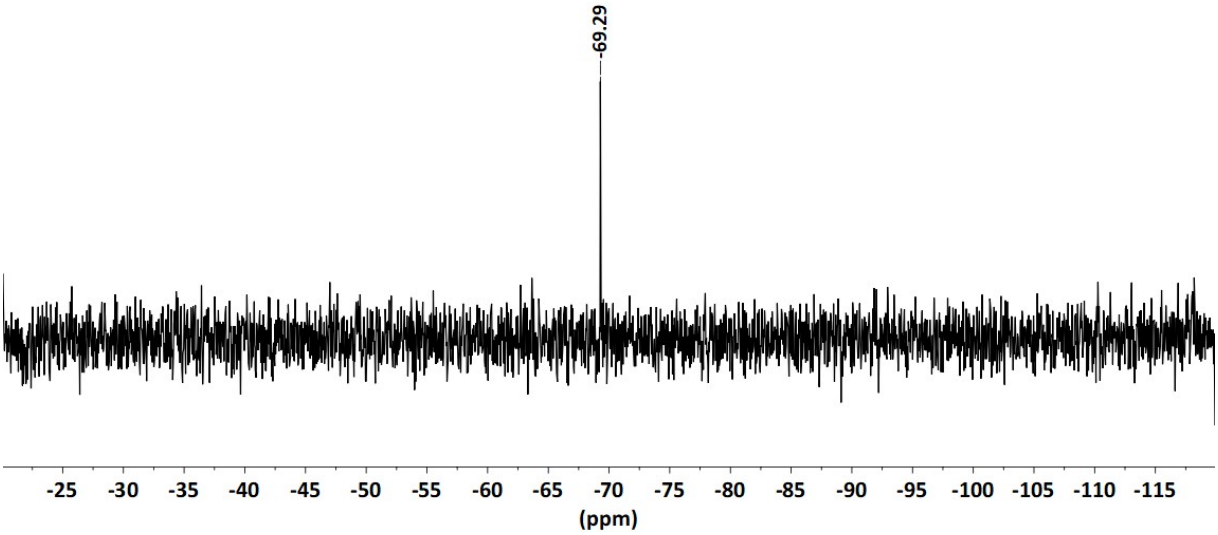

Figure S29. $^{29}Si–\{^{1}H\}–NMR$ spectrum (119.3 MHz, $CDCl_3$)of $\{[(3,5\text{-}(CF_3)_2C_6H_3)_3CO]SiCl_2\}_2O$ (**3b**).

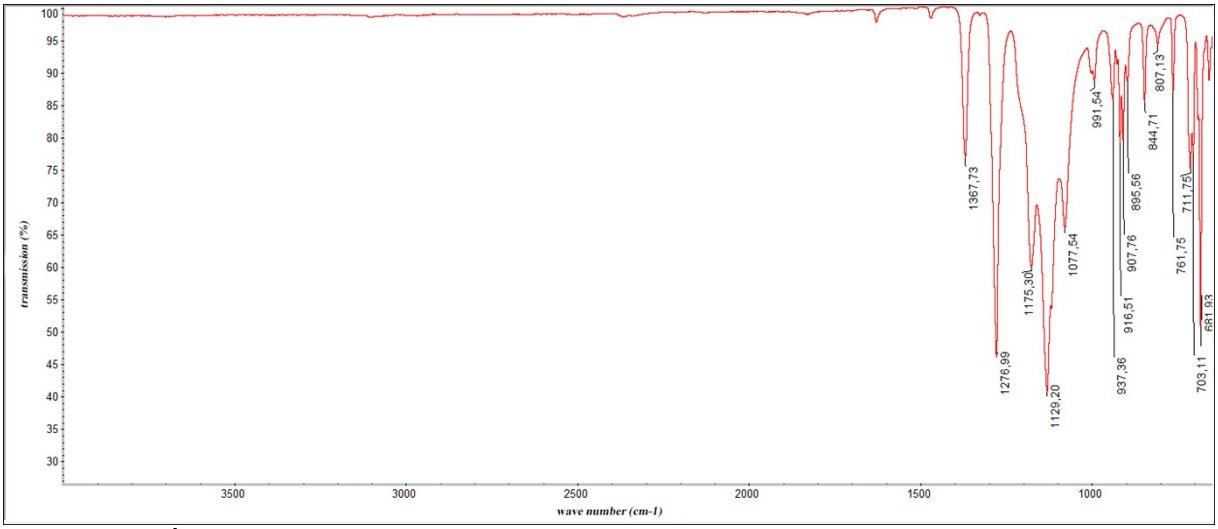

Figure S30. ÍR spectrum (neat) of $\{[(3,5\text{-}(CF_3)_2C_6H_3)_3CO]SiCl_2\}_2O$ (**3b**).

Characterization of $\{[(F_5C_6)_3CO]Si(OH)_2\}_2O$ (4a·Et_2O).

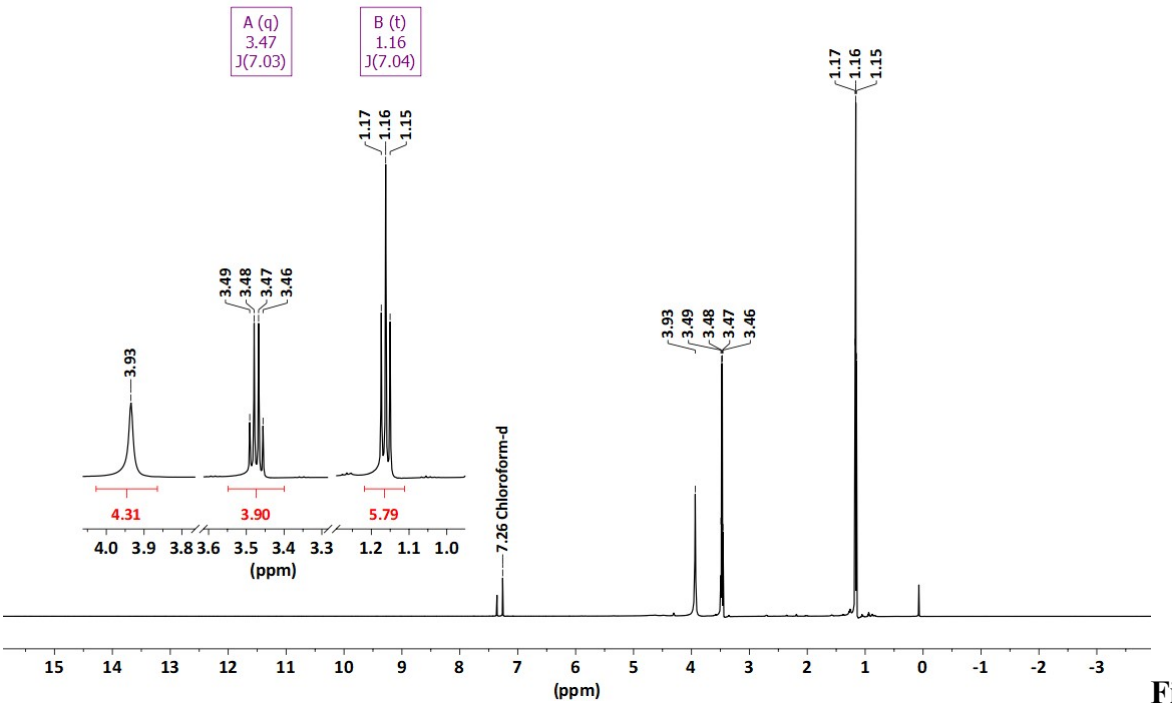

Figure S31. ^{1}H–NMR (600.2 MHz, $CDCl_3$) spectrum of $\{[(F_5C_6)_3CO]Si(OH)_2\}_2O\cdot Et_2O$ (**4a**·Et_2O).

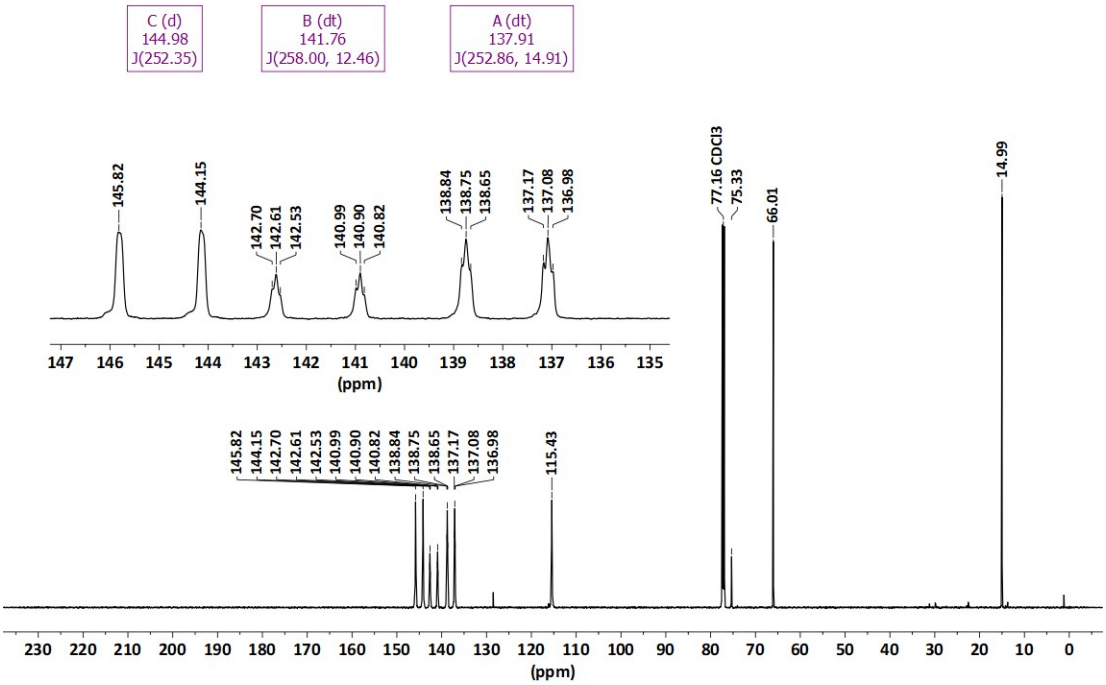

Figure S32. $^{13}C–\{^{1}H\}–NMR$ spectrum (150.9 MHz, $CDCl_3$) of $\{[(F_5C_6)_3CO]Si(OH)_2\}_2O\cdot Et_2O$ (**4a**·Et_2O).

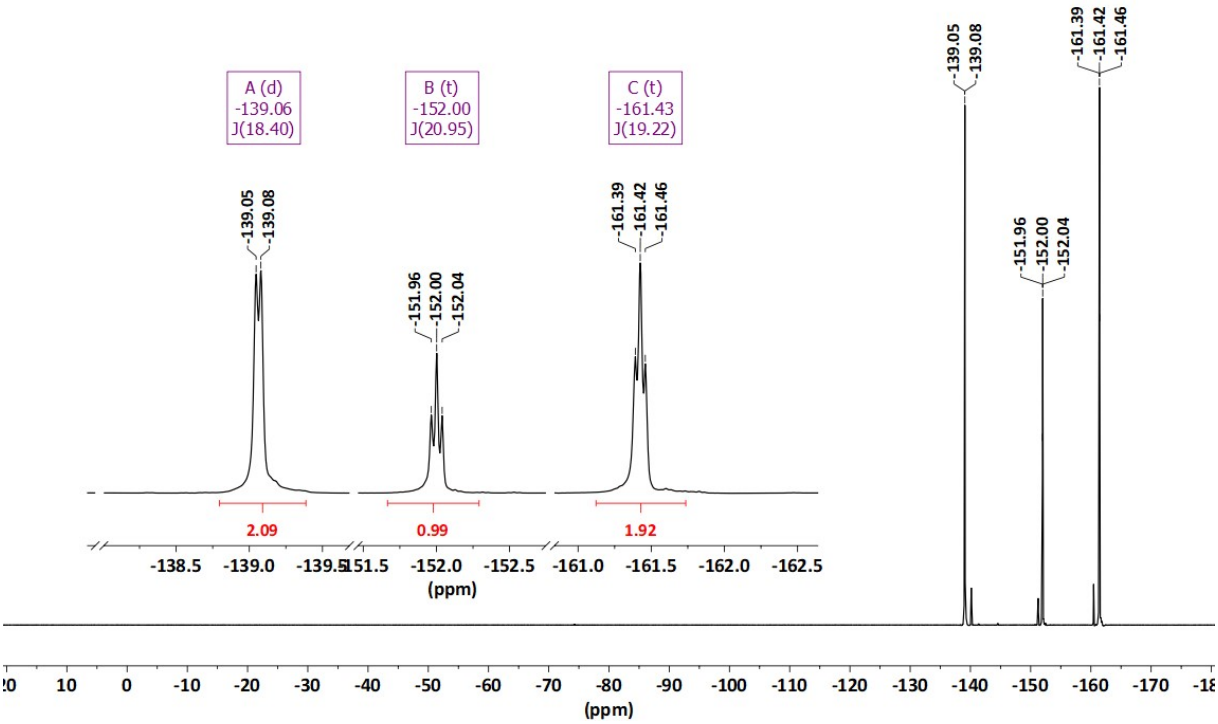

Figure S33. $^{19}F–NMR$ spectrum (564.7 MHz, $CDCl_3$) of $\{[(F_5C_6)_3CO]Si(OH)_2\}_2O\cdot Et_2O$ (**4a**·Et_2O).

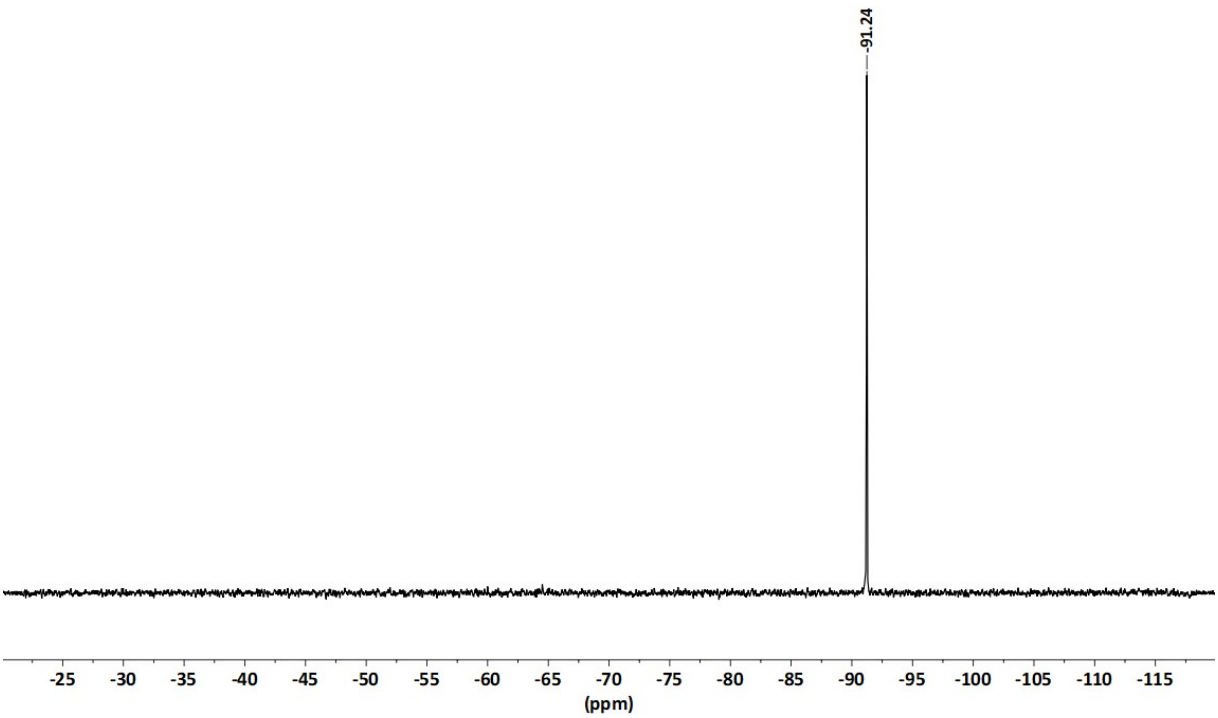

Figure S34. $^{29}Si–\{^{1}H\}–NMR$ (119.3 MHz, $CDCl_3$) spectrum of $\{[(F_5C_6)_3CO]Si(OH)_2\}_2O\cdot Et_2O$ (**4a**·Et_2O).

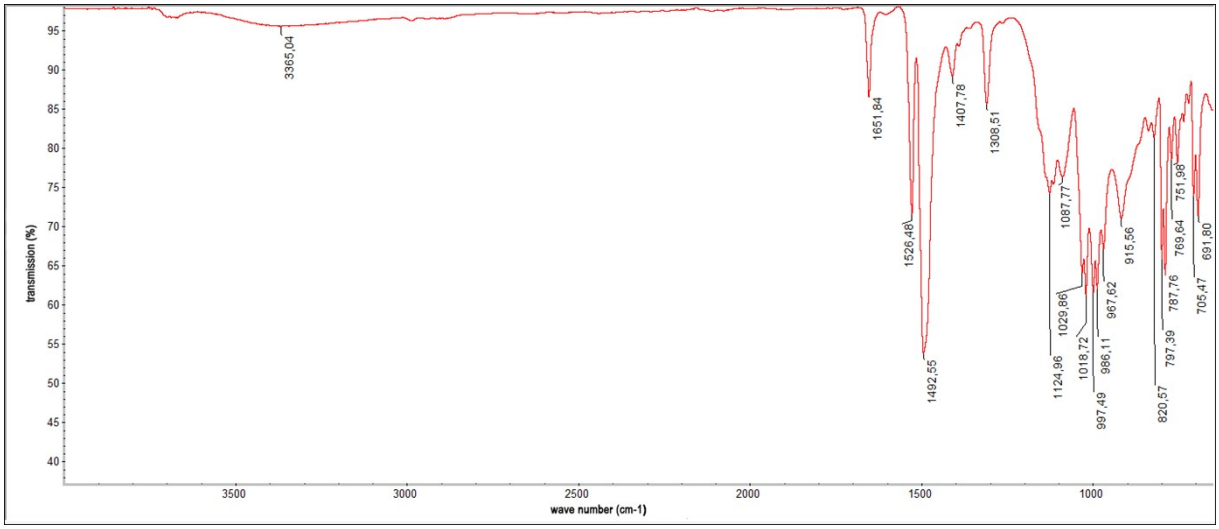

Figure S35. IR spectrum (neat) of $\{[(F_5C_6)_3CO]Si(OH)_2\}_2O\cdot Et_2O$ (**4a**·Et_2O).

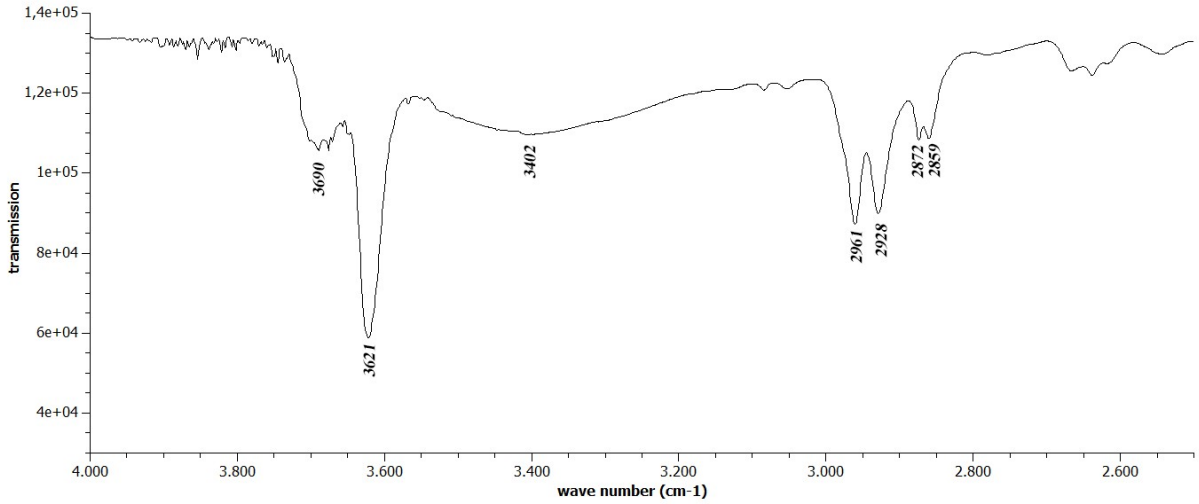

Figure S36. IR spectrum (sample dissolved in CCl_4, c = 20 mg mL^{-1}) of $[(F_5C_6)_3COSi(OH)_2]_2O \cdot Et_2O$ (**4a**·Et_2O).

Characterization of [{(3,5-$(CF_3)_2C_6H_3)_3CO$}$Si(OH)_2]_2O\cdot Et_2O$ (4b·Et_2O).

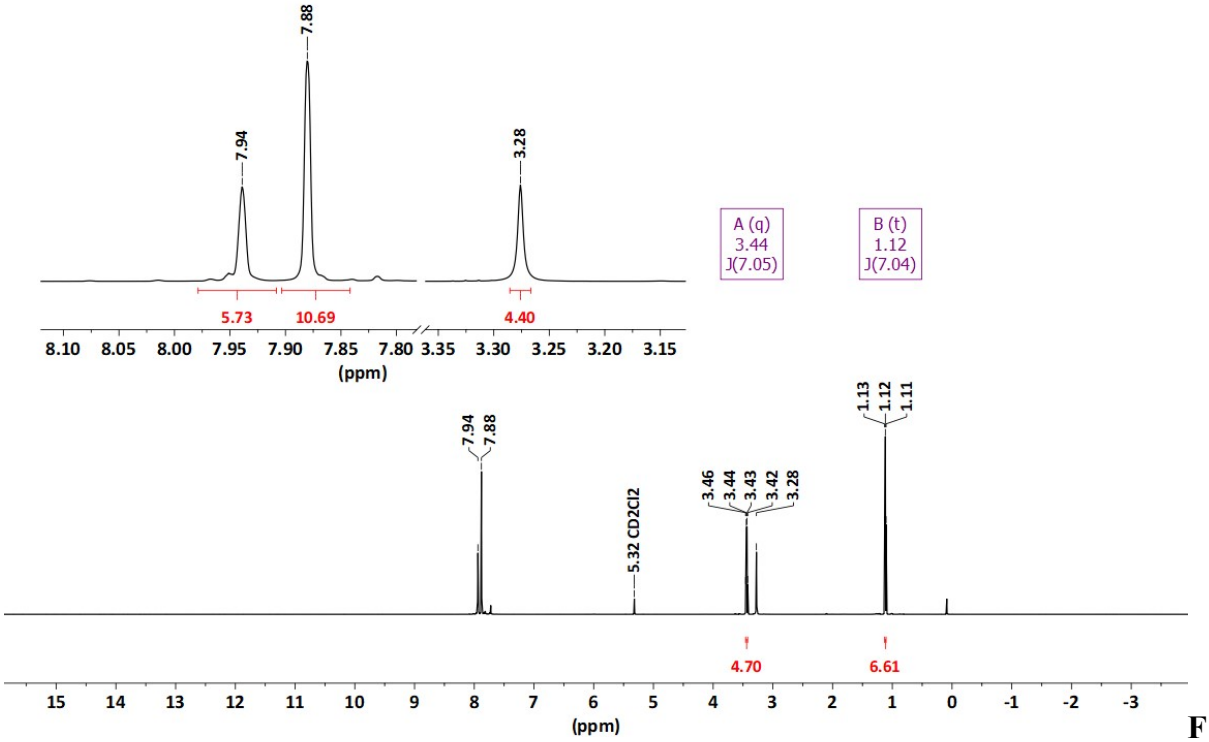

Figure S37. ^{1}H–NMR spectrum (600.2 MHz, CD_2Cl_2) of {[(3,5-$(CF_3)_2C_6H_3)_3CO$]$Si(OH)_2$}$_2O\cdot Et_2O$ (**4b**·Et_2O).

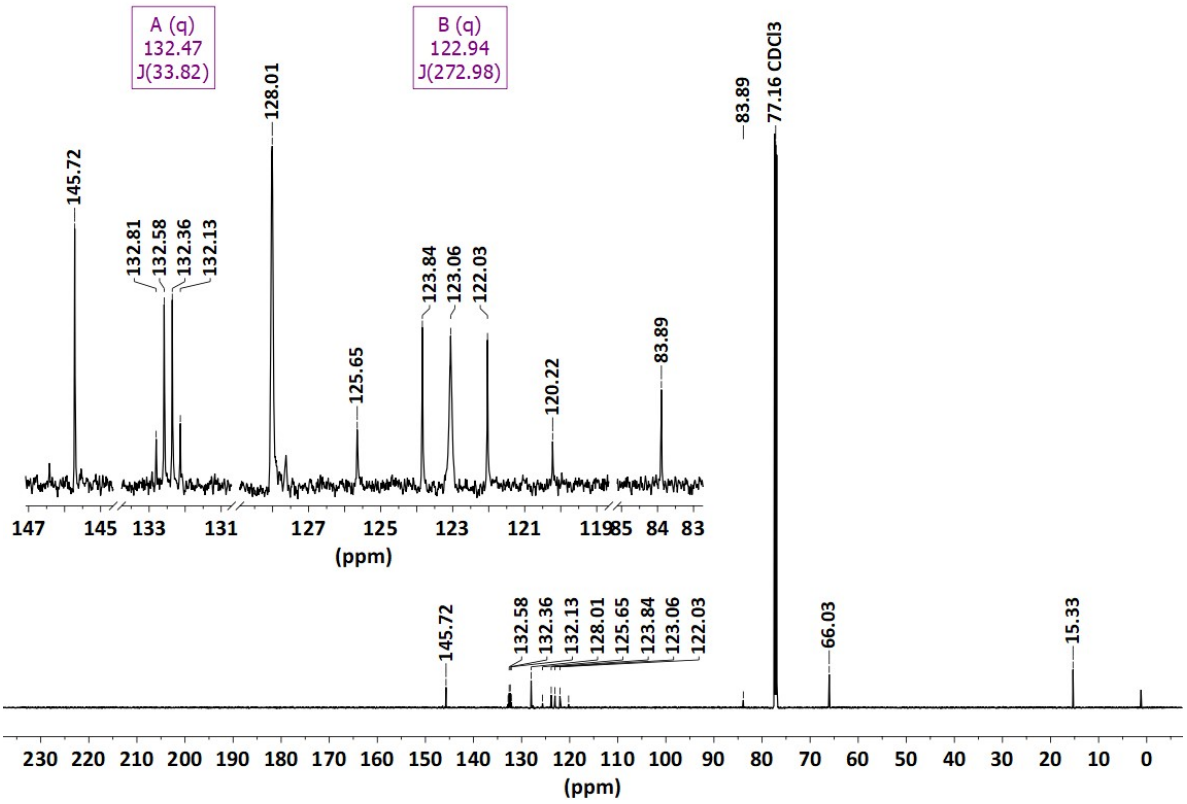

Figure S38. $^{13}C–\{^{1}H\}–NMR$ spectrum (150.9 MHz, $CDCl_3$) of $\{[(3,5\text{-}(CF_3)_2C_6H_3)_3CO]Si(OH)_2\}_2O\cdot Et_2O$ (**4b**$\cdot Et_2O$).

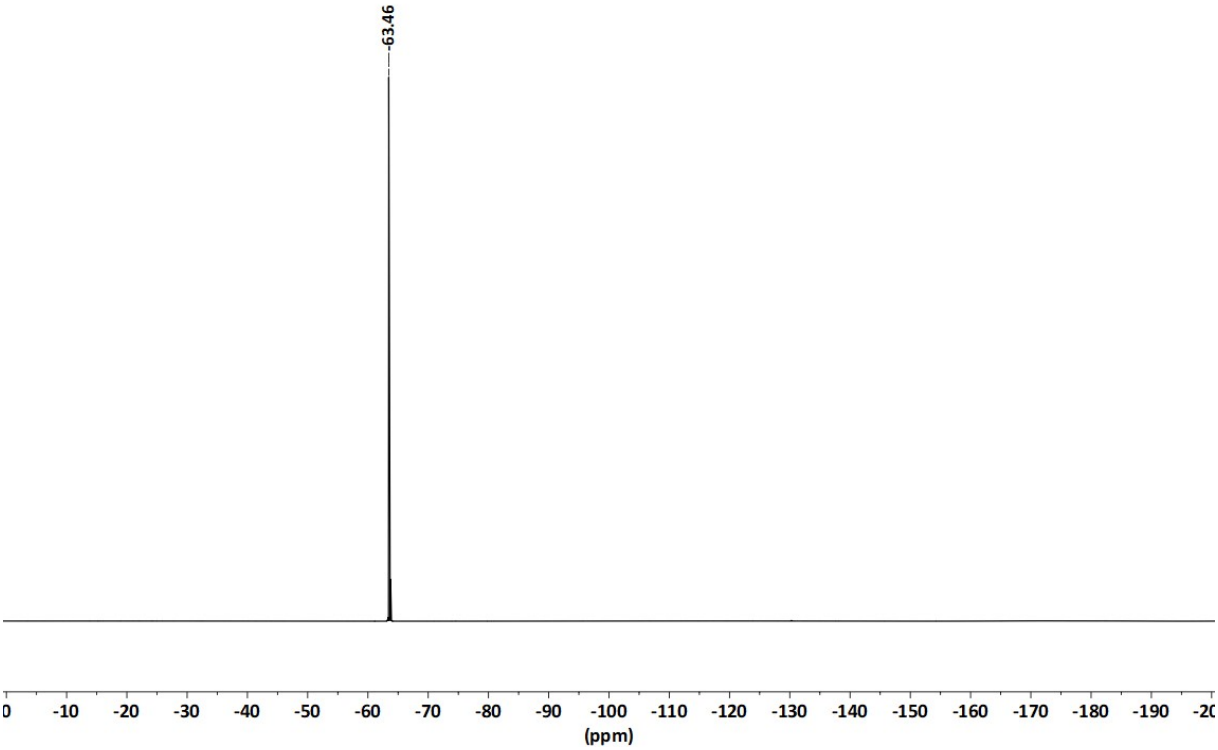

Figure S39. $^{19}F–NMR$ spectrum (564.7 MHz, $CDCl_3$) of $\{[(3,5\text{-}(CF_3)_2C_6H_3)_3CO]Si(OH)_2\}_2O\cdot Et_2O$ (**4b**$\cdot Et_2O$).

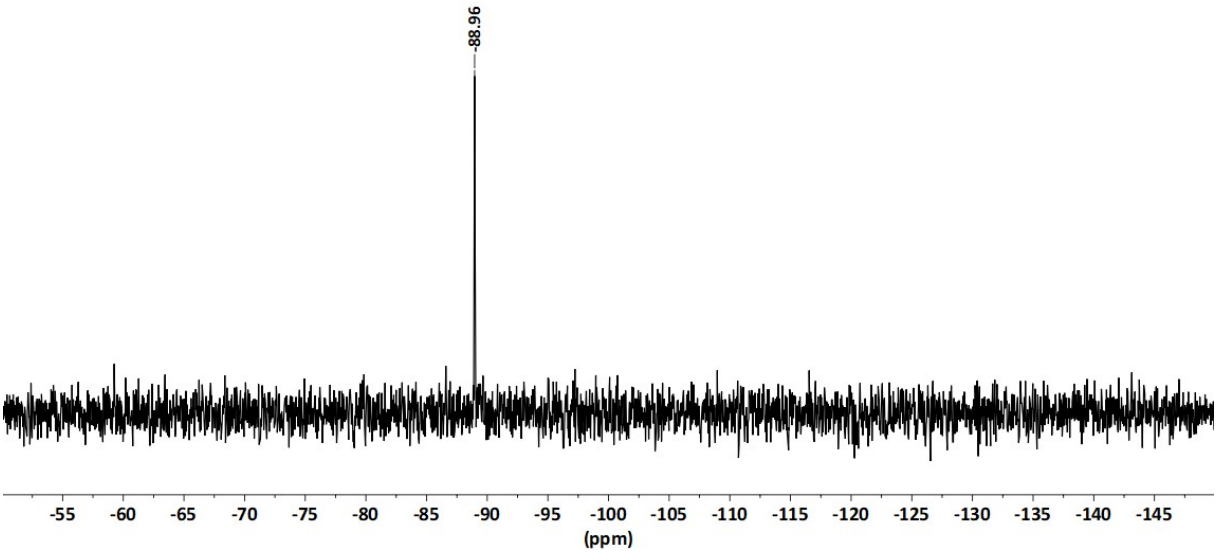

Figure S40. ^{29}Si–{^{1}H}–NMR spectrum (119.3 MHz, $CDCl_3$) of {[(3,5-$(CF_3)_2C_6H_3)_3CO$]$Si(OH)_2$}$_2O\cdot Et_2O$ (**4b**$\cdot Et_2O$).

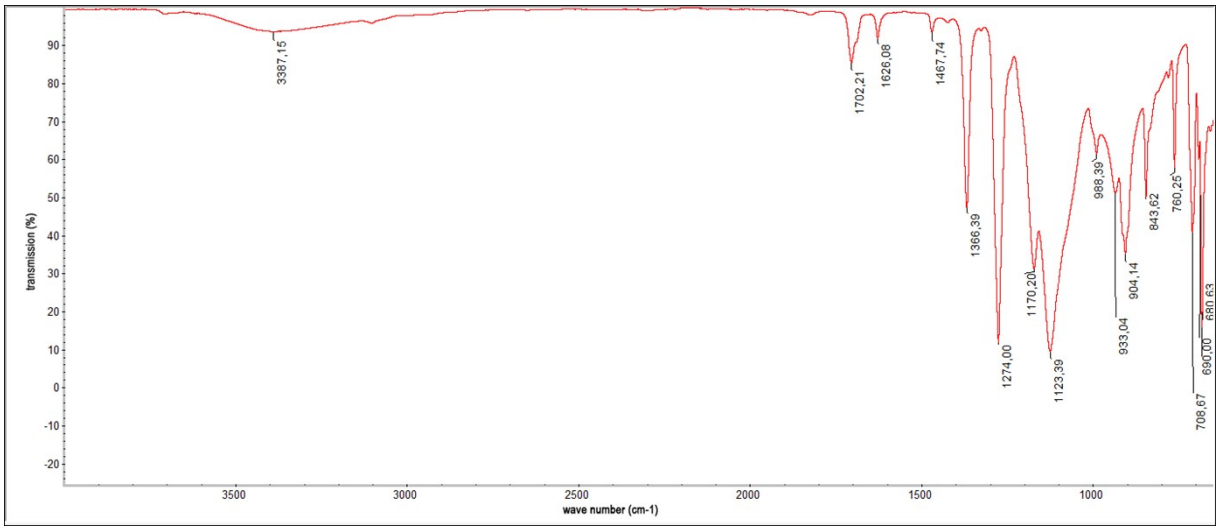

Figure S41. IR spectrum (neat) of {[(3,5-$(CF_3)_2C_6H_3)_3CO$] $Si(OH)_2$}$_2O\cdot Et_2O$ (**4b**$\cdot Et_2O$).

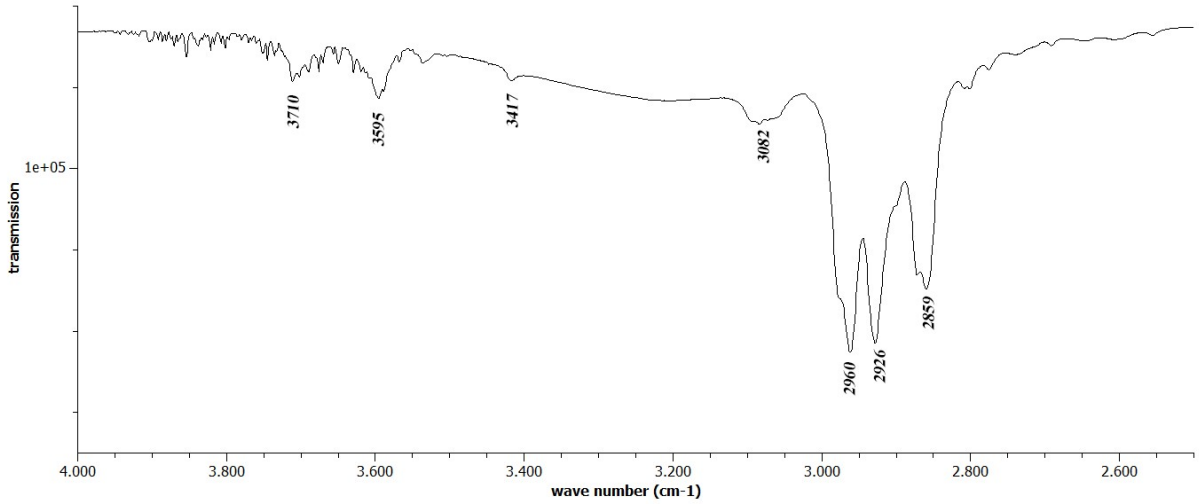

Figure S42. IR spectrum (sample dissolved in CCl_4, c = 20 mg mL^{-1}) of {[(3,5-$(CF_3)_2C_6H_3]_3COSi(OH)_2\}_2O\cdot Et_2O$ (**4b**·Et_2O)

Thermogravimetric Analysis

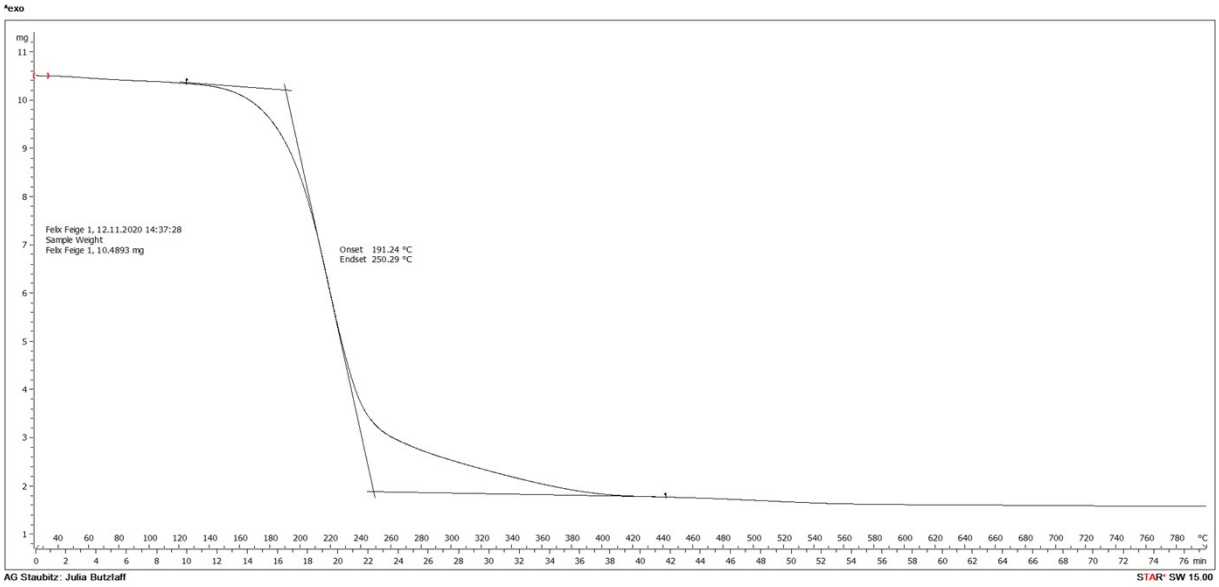

Figure S43. TGA spectrum of $[(F_5C_6)_3CO]Si(OH)_3$ (**2a**).

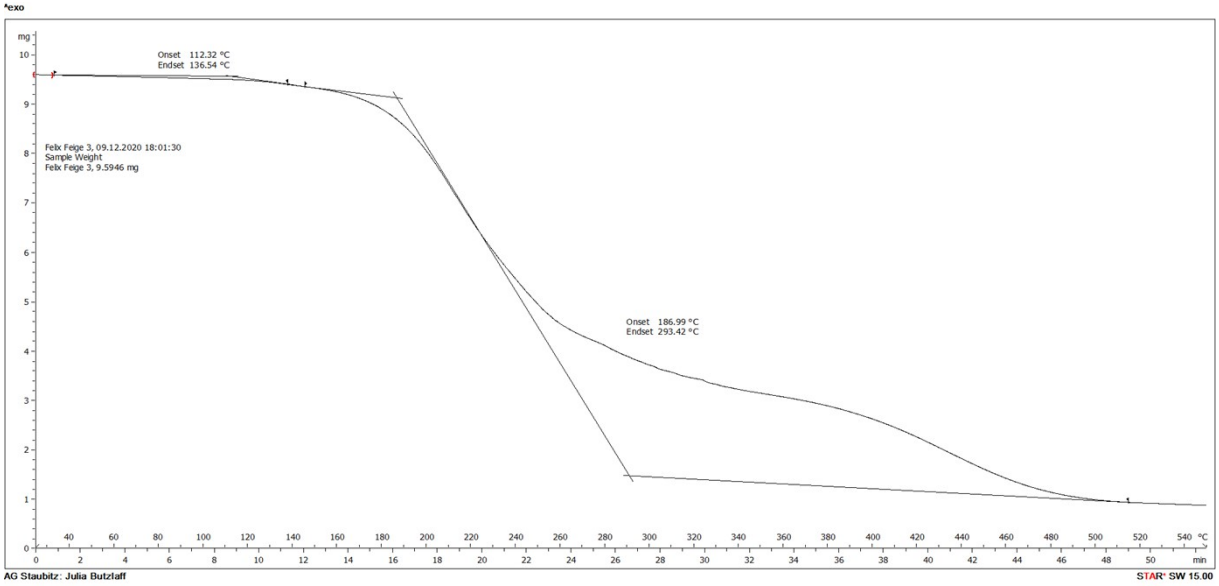

Figure S44. TGA spectrum of $\{[3,5\text{-}(CF_3)_2C_6H_3]_3CO\}Si(OH)_3$ (**2b**).

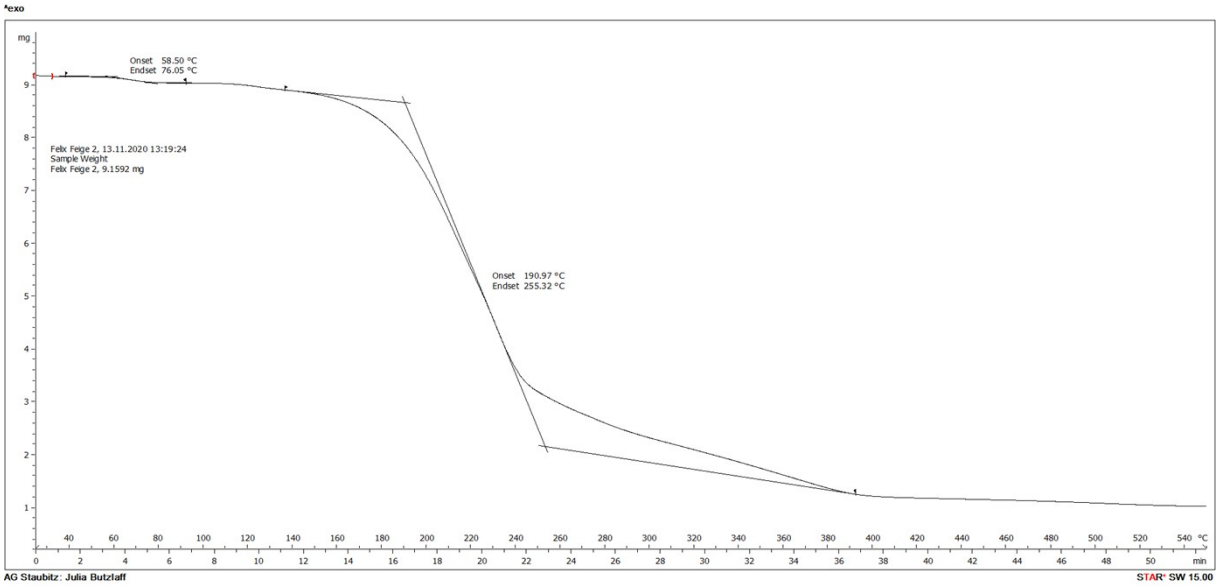

Figure S45. TGA spectrum of $[(F_5C_6)_3COSi(OH)_2]_2O{\cdot}Et_2O$ (**4a**$\cdot Et_2O$).

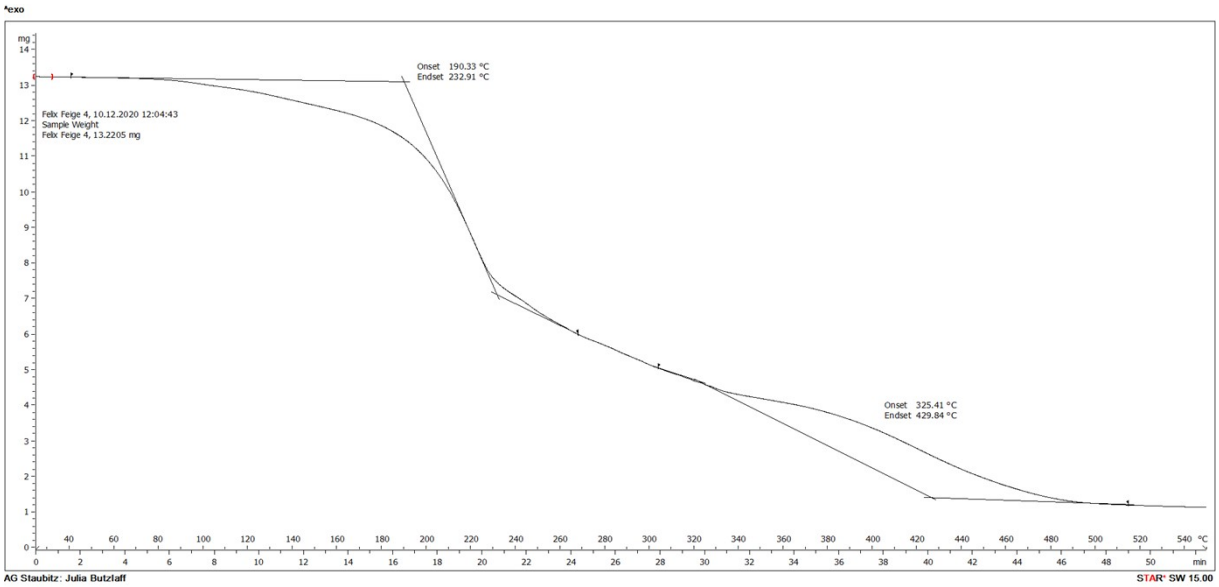

Figure S46. TGA spectrum of $\{[(3,5\text{-}(CF_3)_2C_6H_3]_3COSi(OH)_2\}_2O{\cdot}Et_2O$ (**4b**$\cdot Et_2O$).

Crystallographic data

Table S1. Crystal data and structure refinement of **1a**, **1b** and **2a**.

	1a	**1b**	**2a**·½ C_6H_6·½ Et_2O
Formula	$C_{19}Cl_3F_{15}OSi$	$C_{25}H_9Cl_3F_{18}OSi$	$C_{48}H_{22}F_{30}O_9Si_2$
Formula weight, g mol^{-1}	663.63	801.76	1368.83
Crystal system	triclinic	monoclinic	monoclinic
Crystal size, mm	0.30 × 0.20 × 0.20	0.20 × 0.20 × 0.05	0.30 × 0.20 × 0.10
Space group	$P\bar{1}$	$P2_1/n$	$P2_1/c$
a, Å	11.0941(6)	11.9614(7)	12.0975(4)
b, Å	11.1405(7)	14.8057(8)	26.7831(9)
c, Å	11.2786(8)	16.808(1)	15.9648(5)
α, º	60.792(2)	90	90
β, º	63.338(2)	95.266(2)	101.201(1)
γ, º	65.129(2)	90	90
V, Å^3	1050.41(12)	2964.1(3)	5074.2(3)
Z	2	4	4
ρ_{calcd}, Mg m^{-3}	2.098	1.797	1.792
μ (Mo $K\alpha$), mm^{-1}	0.641	0.485	0.238
F(000)	4134	1576	2720
θ range, deg	2.17 to 33.24	2.19 to 26.39	2.32 to 30.60
Index ranges	–17 ≤ h ≤ 17	–14 ≤ h ≤ 15	–16 ≤ h ≤ 16
	–17 ≤ k ≤ 17	–14 ≤ k ≤ 18	–35 ≤ k ≤ 35
	–17 ≤ l ≤ 17	–21 ≤ l ≤ 21	–21 ≤ l ≤ 21
No. of reflns collected	36091	52041	285954
Completeness to θ_{max}	99.9%	99.9%	99.9%
No. indep. Reflns	8044	6101	12569
No. obsd reflns with($I>2\sigma(I)$)	7089	4081	10810
No. refined params	352	433	810
GooF (F^2)	1.043	1.071	1.073
R_1 (F) ($I > 2\sigma(I)$)	0.0316	0.0644	0.0486
wR_2 (F^2) (all data)	0.0883	0.1193	0.1311
Largest diff peak/hole, e Å^{-3}	0.683 / –0.727	1.355 / –1.986	1.594 / –0.716

CCDC number	2114061	2114062	2114063

Table S2. Crystal data and structure refinement of **3a**, **4a** and **4b**.

	3a	**4a**	**4b**·OEt_2
Formula	$C_{38}Cl_4F_{30}O_3Si_2$	$C_{38}H_4F_{30}O_7Si_2$	$C_{54}H_{32}F_{36}O_8Si_2$
Formula weight, g mol^{-1}	1272.36	1198.59	1548.97
Crystal system	triclinic	triclinic	monoclinic
Crystal size, mm	0.20 × 0.20 × 0.15	0.30 × 0.30 × 0.20	0.20 × 0.20 × 0.20
Space group	$P\bar{1}$	$P\bar{1}$	$P2_1/n$
a, Å	9.7408(6)	11.0814(13)	13.8065(7)
b, Å	9.8621(5)	13.9764(15)	25.8702(10)
c, Å	11.9048(6)	14.1905(17)	18.0791(8)
α, º	85.373(2)	108.150(4)	90
β, º	78.198(2)	104.185(4)	106.562(2)
γ, º	63.964(2)	100.559(4)	90
V, $Å^3$	1005.80(10)	1942.7(4)	6189.5(5)
Z	1	2	4
ρ_{calcd}, Mg m^{-3}	2.101	2.049	1.662
μ (Mo $K\alpha$), mm^{-1}	0.538	0.292	0.218
F(000)	618	1172	3088
θ range, deg	2.30 to 28.30	1.98 to 28.46	2.19 to 28.29
Index ranges	–12 ≤ h ≤ 12	–14 ≤ h ≤ 14	–18 ≤ h ≤ 18
	–13 ≤ k ≤ 13	–18 ≤ k ≤ 18	–34 ≤ k ≤ 34
	–15 ≤ l ≤ 15	–18 ≤ l ≤ 18	–24 ≤ l ≤ 24
No. of reflns collected	28633	44012	164878
Completeness to θ_{max}	99.9%	99.9%	99.9%
No. indep. Reflns	4964	9698	15340
No. obsd reflns with($I>2\sigma(I)$)	3713	7278	11621
No. refined params	358	698	988
GooF (F^2)	1.029	1.044	1.025
R_1 (*F*) ($I > 2\sigma(I)$)	0.0445	0.0621	0.0597
wR_2 (F^2) (all data)	0.1056	0.1825	0.1610
Largest diff peak/hole, e $Å^{-3}$	0.390 / –0.459	1.032 / –0.733	1.960 / –1.084
CCDC number	2114064	2114065	2114066